Declaration

Acknowledgement

I wish to thank my supervisors Dr. Phil Riches and Dr. Scott Wearing. Dr. Phil Riches conceived the project idea and he guided me in all aspects of the project. I am very thankful for all his support and advice, which helped me undertake the project. Dr. Scott Wearing was also involved in some part of the project such as tissue preparation training, designing the machine and testing the specimens. I would like to thank Prof. Alexander Nicol for giving me the opportunity to join at the Bioengineering Unit of University of Strathclyde.

I am also extremely grateful for all the technical help I received; Davy Robb for building the frame and Dave Smith who supported and trained me for tissue preparation procedures and provided clinical tools for my research.

Finally, I wish to thank my family and friends without their support, I could not have completed my research.

Contents

List of figures

List of tables

Abstract

***Background*:** The size of lesions on articular cartilage are difficult to estimate using conventional preoperative imaging techniques, which may prevent the use of conservative procedures in the restoration of joint function following osteoarthritis (OA). Arthroscopic probes have been designed to be used intraopertively which can assess the mechanical integrity of the cartilage surface. These devices may not have the sensitivity to detect early OA. Therefore, there exists the need for a low load indentation system which can determine both static and time-dependent properties of the tissue and thereby improve the likelihood of early OA detection. Such a probe also has the potential for mounting on a robotic arm for precise excision of tissue. In order to determine the early signs of OA, it is important to characterise the repeatability, variation and mechanical response of the articular cartilage surface to being indented with respect to different experimental parameters.

***Objective*:** To design, build and evaluate a bench top indentation system to assess the viscoelastic properties of articular cartilage, which has the potential to be converted to a device that could be used arthroscopically and intraopertively. In particular, it was the aim to:

- investigate the difference between a spherically headed indenter and a flat headed indenter in assessing the cartilage mechanical properties in vitro;
- evaluate articular cartilage's preconditioning properties by cyclic indentation testing;
- and to evaluate the recovery of articular cartilage subsequent to the preconditioning.

***Methods*:** A bench top materials testing device was designed and built using a high resolution linear actuator and a spring-loaded Linear Variable Differential Transducer (LVDT). The actuator drove the tip of the LVDT, with either a flat or spherical tip, into the cartilage surface and the spring of the LVDT provided a known force and displacement. The surface deformation of the cartilage could then be determined from such a device.
Healthy osteochondral plugs were harvested from the bovine tibial plateau articulating surface using an osteochondral coring tool. Plugs were mounted in plaster of paris with the cartilage surface normal to the indenter. All test procedures were identical: an actuator displacement of 5mm, a ramp speed of 5mm/second and a holding time of 30 seconds.

An initial experiment was performed on a metal plug to ensure that any recorded deformation was that of the cartilage surface and not of the underlying environment. Subsequently the indentation mechanics of two indenter tips was evaluated: a spherical head indenter of diameter 4.8 mm and a flat ended indenter with a diameter of 5.1 mm. Then the cartilage preconditioning properties were evaluated using the flat-ended indenter. Each plug was tested 10 times in exactly the same place on the cartilage surface with a time interval of 20 seconds between each test. Finally, to test how long the cartilage takes to recover from its preconditioned state, each plug was indented 5 times in exactly the same place on the cartilage surface with a time interval of 20 seconds between each test and a further 6th indentation was also done in the same place on the cartilage surface but after either 1, 5, 10, 20 or 30 minutes interval. This 6^{th} result was compared to the initial indentation. If the properties determined from the 6^{th} indentation were the same as those of the first indentation, one could say that the sample had recovered.

***Results*:** Indenting the metal plug did not result in any measurable deformation indicating that subsequent measures are that of the cartilage surface and not of any underlying structures. When indenting with the spherical head indenter the deformation was deeper and quicker than using the flat-ended indenter due to the small contact region on the cartilage surface which means that there was higher stress on the surface compared with the flat-ended indenter.

The preconditioning experiment indicated that the indentation depth decreased with each cycle of loading until approximately the 5^{th} cycle after which the cartilage may be assumed to be preconditioned, since successive indentations exhibited similar mechanical behaviour. The time constant describing the surface deformation with time did not undergo any preconditioning which means that only the stiffness is affected by preconditioning, not permeability. Thirty minutes of recovery was sufficient for the surface to fully recover to its original state.

***Conclusions*:** A bench top device has been designed and manufactured that can assess the mechanical characteristics of articular cartilage. Furthermore, this device has demonstrated mechanical differences in the surface response between indenter geometries and the preconditioning and recovery characteristics of cartilage. Suggestions and comments have

been made regarding the next phase of this research into the development an arthroscopic indentation device.

1. General introduction

1.1. Joint pain and articular cartilage

Joint pain is a serious condition affecting people of all age groups, but particularly in older people and highly active men and women. Those affected suffer from chronic pain, joint stiffness, tenderness and ultimately disability, often due to the degeneration of articular cartilage. Degeneration of articular cartilage and the underlying subchondral bone is termed osteoarthritis, for which age, joint injury, obesity and misalignment are some of the well-known risk factors (Felson et al., 1987). An estimated 15% (40 million) of Americans had some form of arthritis in 1995. In the United States the approximate number of people suffering from arthritis will increase to 18.2% (59.4 million) by 2020 and by 2050 approximately 60 million Americans will suffer from arthritis (Lawrence et al., 1998). The osteoarthritis incidence and progressive rates are 2.5% and 3.6% per year, respectively (Cooper et al., 2000). Osteoarthritis increases with age and women are at a higher risk (4.9%) than men (2.6%). The relative risk for women compared with men increased from 1.57 at 45-54 years to 2.14 at 65-74 years (Davis et al., 1988).

Nowadays there are plenty of surgical treatment methods available to treat osteoarthritis such as total knee arthroplasty (TKA) (Nesic et al., 2006), transplantation of osteochondral autografts (Mosaicplasty) (Whiteside et al., 2005; Hangody and Fules, 2003; Hangody et al., 2004) and the micro fracture technique (Mithoefer et al., 2005). The main hindrance to conservative treatments being that articular cartilage has a limited capacity for regeneration (Buckwalter and Mankin, 1997; Hunziker., 1999). Therefore, presently, the main treatment for osteoarthritis affected joints is arthroplasty. The main limitations of the arthroplasty treatment are the currently used material does not have the ability to withstand patient's physical activities, loosen and occasionally break (Nesic et al., 2006). Nevertheless, another successful treatment for chondral and osteochondral defects is Autologous Osteochondral Mosaicplasty. Mosaicplasty is a operation of creating an osteochondral autograft by harvesting and transplanting many small cylindrical osteochondral plugs (2.7, 3.5, 4.5, 6.5, 8.5 mm in diameter) from the minimal weight-bearing periphery of the patellofemoral joint and transplanting them into drilled tunnels in the defective weight-bearing surface such as knee and

other synovial joints. Combination of different osteochondral plug sizes allow a 90% to 100% defect-filling rate (Hangody and Fules, 2003; Hangody et al., 2004). In order to do this determining and quantifying the extent of the osteoarthritis interoperatively by a manner other than visual inspection would be highly useful to identify the total region of arthritis. So there is an immediate need for orthopaedic surgeons to assess the cartilage quality in vivo that does not damage the specimen.

Arthroscopic indentation techniques, whereby a probe assesses the mechanical properties of the articular cartilage intraoperatively, may facilitate the identification of areas of, and the extent of, degenerated cartilage, thereby allowing more conservative treatments to be used. However, current arthroscopic indentation techniques utilise the elastic properties of cartilage (Imer et al., 2006), which may not be the best parameter for the identification of such areas. This thesis concerns a novel design of indentation system that may be able to determine the viscoelastic parameters of cartilage which may be more prone to vary with degeneration.

1.2. Aims of the study

The aims of this thesis are as follows:

- To design, build and evaluate a bench top indentation system to assess the viscoelastic properties of articular cartilage, which has the potential to be converted to a device that could be used arthroscopically and intraopertively. This device may then be as an alternative to more expensive tissue testing equipment.

And using the above indentation system:

- To investigate the difference between a spherically headed indenter and a flat headed indenter in assessing the cartilage mechanical properties in vitro.
- To evaluate the preconditioning properties of cartilage by cyclic indentation testing.
- And to evaluate the recovery of articular cartilage subsequent to the preconditioning.

1.3. Thesis structure

A detailed literature review about articular cartilage is presented in chapter 2, this includes cartilage and its types, composition, structure, mechanical properties, regeneration, indentation on the cartilage surface, preconditioning and recovery properties. The connection between literature gaps and this thesis aims are highlighted in the subsequent research question section.

In chapter 3, the bench top material testing machine design, working procedure and electronics parts working protocol has been explained. The programming method and control systems has been explained in chapter 4 which includes the program working format, flow chart and working principle both in calibration of instrument and during cartilage measurement. The experimental methodology is presented discussed in chapter 5 along with the osteochondral plug preparation procedure. Chapter 6 describes the experimental methods for all experiments such as indenting on a metal plug, the comparison of spherical head and plane head indenters and preconditioning and recovery of cartilage. All experiment obtained results and data analysis were explained in chapter 7, along with diagrams under the title of results. In chapter 8, discussions of all experiments were based on the results and methods, conclusion and possibilities for future work. Chapter 9 contains the references which have been cited elsewhere in the thesis. Finally, chapter 10 contains engineering drawings of the machine and the matlab programming code.

Except where indicated in the text the work is that of the author, specifically, designing and construction of apparatus using components sourced by the author's supervisor, all experimental work and analysis of data.

2. Literature review

2.1. Introduction

Cartilage is a connective tissue with unique functional properties covering the surfaces of the bone, ears, nose, rib cage and in the body (Barbucci, 2002, Hunziker, 2001). Cartilage consists of a combination of water, chondrocytes, non-fibrous filler substance (carbohydrate and non-collagenous proteins), collagen fibres (type I and II) and proteoglycans (Bullough and Goodfellow, 1968). These combine and form a matrix which is a very flexible and durable tissue which can be 0.5 to 5 mm thick. There are three types of cartilage: fibro cartilage, elastic cartilage and articular cartilage,

2.1.1. Fibro cartilage – Fibro cartilage contains a larger amount of non-collagenous proteoglycan than the other types of cartilage and typically the collagen is arranged in layers. It is also white and has a high tensile strength and is highly compressible. It is predominantly present in intervertebral discs and ligaments (Marieb and Hoehn, 2007).

2.1.2. Elastic cartilage – Elastic cartilage contains a larger proportion of elastic fibres than the other types of cartilage, which provides more elastic strength. It is yellow in colour and predominantly found in pinna of the ears, epiglottis, nose and mouth (Hutmacher et al. 2003).

2.1.3. Articular cartilage – Articular cartilage (also called hyaline cartilage) is a white avascular, alymphatic, aneural tissue and the most prevalent type of cartilage in adults. It is found in ears, nose, smaller respiratory tubes and mainly at the joint surfaces of articulating bones (Trattnig, 1997) for example, the knee (Figure 2.2). Articular cartilage will be discussed in detail in section 2.3.

2.2. Osteoarthritis

Arthritis is a common term used to describe the pain in the joints and osteoarthritis is one of the most common diseases affecting human joints (Redman et al., 2005). Osteoarthritis is one of the most prevalent diseases in orthopaedics and worldwide many people suffer from osteoarthritis (Felson, 1990). The main pathological feature of osteoarthritis is the loss of articular cartilage (Felson, 2004). Osteoarthritis is a most common form of arthritis which

creates pain in the knee and hip joint. Osteoarthritis degenerates the tissues slowly and eventually leads to the painful rubbing of bone on bone in the joint. Unfortunately, articular cartilage has a limited self repairing capacity due to the fact that there are no blood vessels in the tissue (Lorenz and Richter, 2006).

The major issue of osteoarthritis research is that the disease is mostly not diagnosed until the joints lead to pain and radiographically detectable changes in cartilage surface. Early stage osteoarthritis is very difficult to clinically diagnose. Good articular cartilage has a smooth and glittering surface without fissures. But at the beginning of the cartilage degeneration process some changes can be detected in the cartilage surface which is fissures on the surface and the lack of a smooth surface. In more advanced osteoarthritis, the cartilage surface is completely broken-down with plenty of fissures and cracks which can reach up to the calcified zone of the cartilage (Veje et al., 2003) (Figure 2.1).

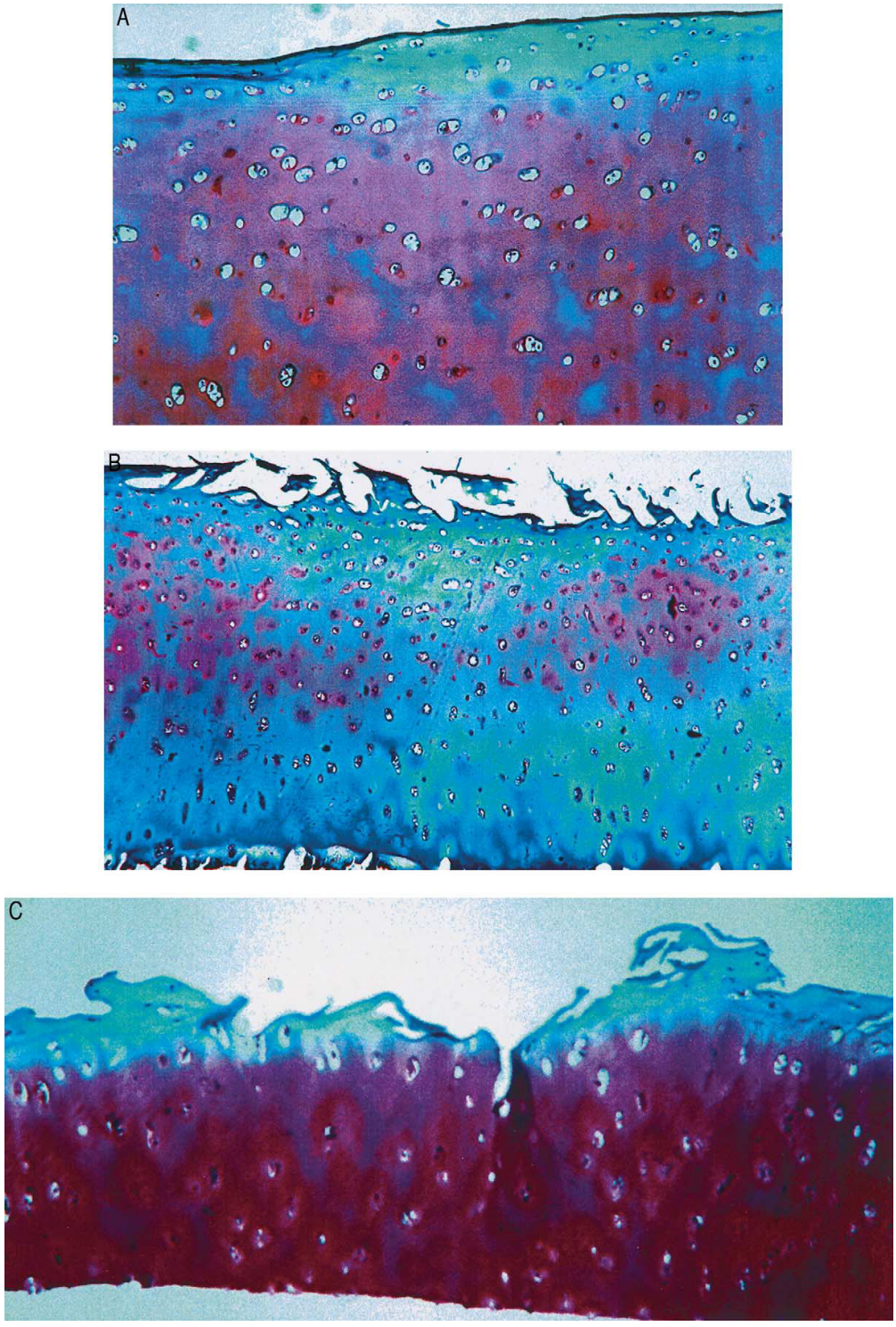

Figure 2.1: (A) Normal articular cartilage. (B) Articular cartilage with mild Osteoarthritis showing mild fibrillation at the entire surface. (C) Articular cartilage with advanced osteoarthritis showing more advanced fibrillation, a fissure through the superficial zone. Image taken from (Veje et al., 2003).

2.2.1. Repair and regeneration

Articular cartilage has limited capacity for self repair or regeneration. This is due to articular cartilage being an avascular tissue and with little cell mobility due to the surrounding matrix (Hunziker., 1999). Furthermore due to the extracellular matrix, chondrocytes cannot migrate to damaged areas (Francisco Forriol., 2009). Nutrition is supplied through the synovial liquid by diffusion (Newman. 1998). In the normal physiological condition articular cartilage will lubricate by itself, however, if the tissue becomes damaged, this can disturb the self lubrication process which further damages the tissue through increased wear. Therefore if cartilage gets damaged it is very difficult to remedy the situation.

2.3. Articular cartilage

To understand osteoarthritis better, the structure-function relationship of articular cartilage needs to be detailed. This is the purpose of this section.

Articular cartilage is an important component in synovial joints such as the knee and the hip to reduce the friction. A loss of mechanical integrity of articular cartilage may be related to osteoarthritis and joint pain. Articular cartilage (Figure 2.2) is an elastic soft white smooth glistening tissue which is found mainly on the articulating surfaces of the bones like the femur and tibia (Wayne. 2008, Federico et al., 2004). Articulating joints require smooth movement between the bones and articular cartilage an extremely low coefficient of friction which provides this smooth motion at joints. When the joints are impacted the cartilage distributes the load to the whole body through the bones (Schachar et al., 1999).

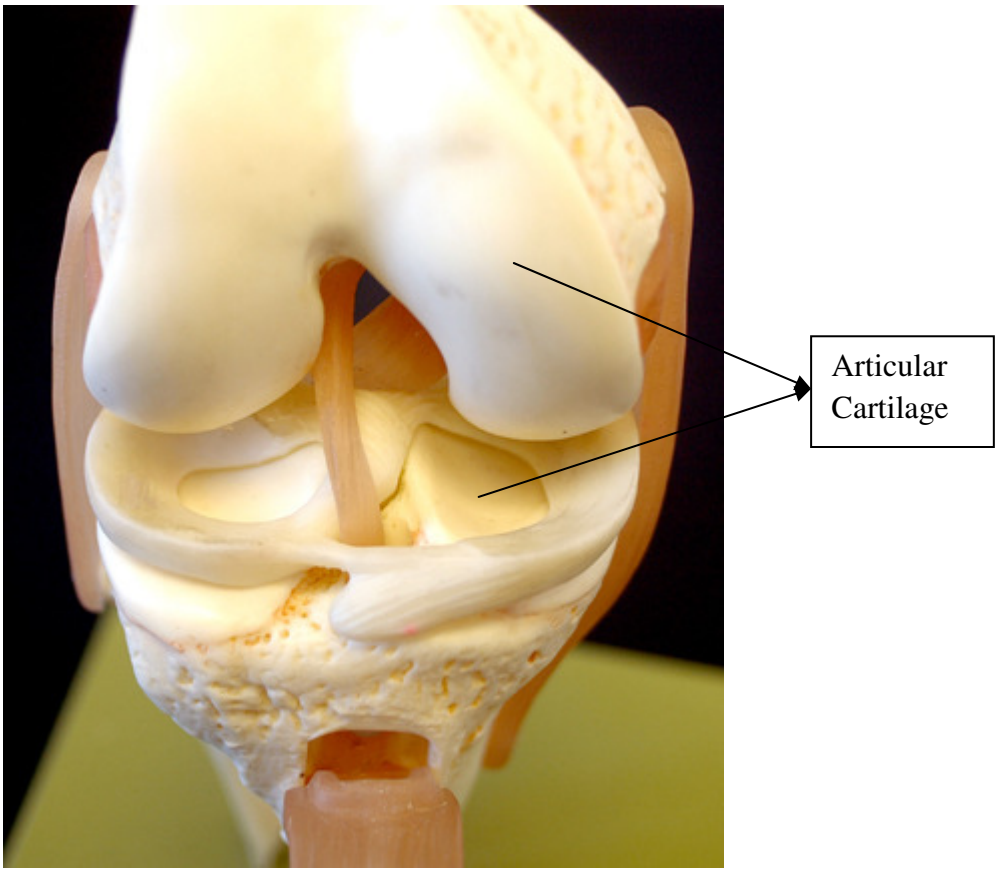

Figure 2.2: Location of Articular Cartilage. Image copied from (http://cartilagetear.com/).

2.3.1. Articular cartilage composition

Articular cartilage consists of water (75-80%) and a solid matrix (20-25%) (Wu and Herzog 2002). The solid matrix of articular cartilage made up of collagen fibres (65%), proteoglycan gel (25%), chondrocytes (<10%) and lipids (<10%) (Eyre, 1990) (Figure 2.3). These constituents are described in more detail in the following sections.

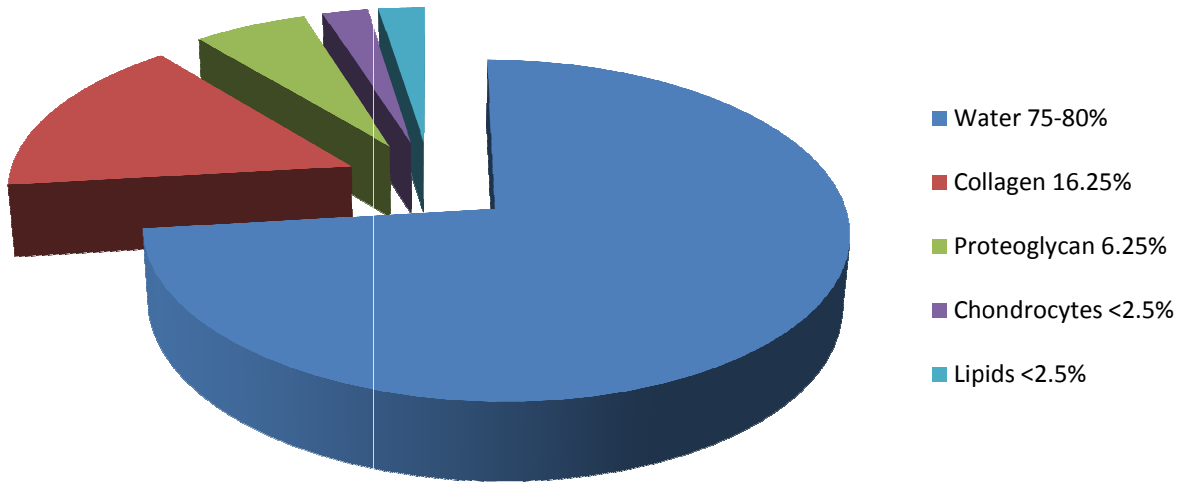

Figure 2.3: Composition of the solid component of the extracellular matrix in articular cartilage.

2.3.2. Structure of articular cartilage

Articular cartilage collagen orientation is parallel to the surface of the cartilage and perpendicular to the deeper zone. The chondrocytes cells form as columns, situated parallel to the collagen fibres in the middle and deep zones. Throughout the thickness of the cartilage the collagen fibres and proteoglycans are arranged differently: there is more collagen at the joint surface and more proteoglycans in the calcified layer. This arrangement helps to mechanically withstand the large tensile stresses at the cartilage surface at the edges of the contact areas. The compressive stress is found in the deeper zone of the cartilage which is resisted by hydrostatic pressure in the water.

The whole cartilage thickness is 0.5 mm to 5mm depending the age of the person. The meniscus is the 'C' shaped thin layer; it is a specific portion of the knee cartilages which is partly divided by the joints. The two menisci act as a shock absorber to absorb the impact and also assure smooth movements and stability of the knee structure. Synovial fluid lubricates the joint and helps to transfer nutrients to the articular cartilage. The articular cartilage looks like a solid homogenous material at the level of between 0.1mm and 1 cm. And between 0.1 microns and 0.1 mm level of the structure is called micro structure. In this level the articular cartilages consist of the chondrocytes and the organization of the type II collagen. The organization at this level can be divided into four zones.

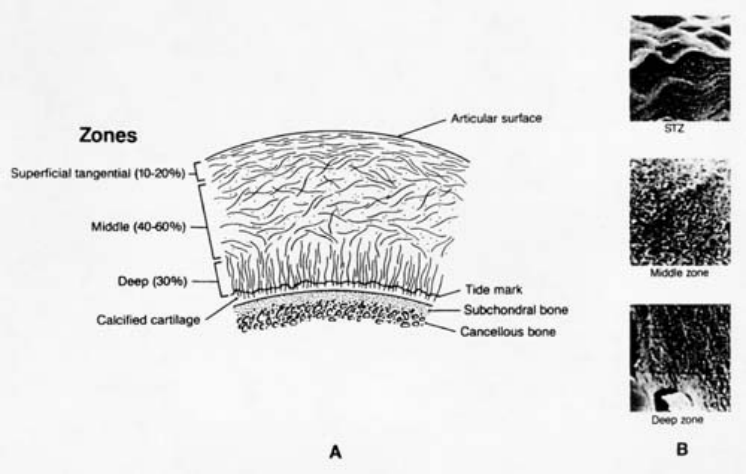

Figure 2.4: Articular cartilage zones (www.engin.umich.edu).

The structure of articular cartilage can be described as series of zones is between the surface of the articular cartilage and the subchondral bone (Figure 2.4). The surface of the articular cartilage is the superficial zone and consecutively there are the middle zone, the deep zone and calcified zone; each layer has specific structure and morphology and therefore each zone varies from one another from the degree of tensile strength and stiffness.

The superficial zone is surface of the cartilage. Around 10 - 20% of articular cartilage thickness is superficial zone and it contains the highest volume (85%) of collagen by dry weight. This concentration of collagen correlates with its high tensile strength. The superficial zone is a key mediator of boundary lubricant of articular joints which prevents shear stress, because the

superficial zone reduces the coefficient of friction of the articular surface. The nutrients from synovial fluid are carried out through superficial zone.

The middle zone contains 40 - 60% of the cartilage is strongly built up with collagen fibres. The middle zone contains smaller chondrocytes. Compared with the superficial zone, the middle zone has a higher concentration of proteoglycans and lower collagen. The main function is resisting both shear and compressive stress when it is impacted.

The deep zone is around 30% of the cartilage thickness, containing chondrocytes and a high percentage of proteoglycan. This combination improves the compressive strength of articular cartilage. The collagen fibres are oriented perpendicular to the calcified zone in this zone.

Finally, the calcified zone is the connective zone between non calcified cartilage and subchondral bone.

2.3.3. Chondrocytes

The only cells found in articular cartilage are chondrocytes (Heath and Magar, 1995), with a cellular density less than other tissue such as muscle tissue and nervous tissue (Eyre, 1990). Chondrocytes are located in chambers called lacunae. Sometimes the cells are found in fibrous capsules in the matrix, which are called chondrons. Articular chondrocytes in situ vary in size, shape and concentration according to horizontal zones such as superficial zone, middle zone, deep zone and calcified zone. At the joint surface of the cartilage, chondrocytes are widely scattered through the matrix (Figure 2.5). In the superficial zone the cell density is low and their shape is an elongated oval approximately 10 – 20μm in diameter. In the middle zone the cells are spherical with a diameter of around 10μm and in this zone the chondrocytes present themselves in groups. In the deep zone the group of cells tend to be oriented normal to the surface. The chondrocytes main function is to manufacture and maintain the cartilage matrix with nutrients and waste materials being exchanged between the bloodstream and the cells (Muir, 1995, Martin et al., 1998) and also significantly involves to the mechanical properties of the cartilage (Guilak, 2000).

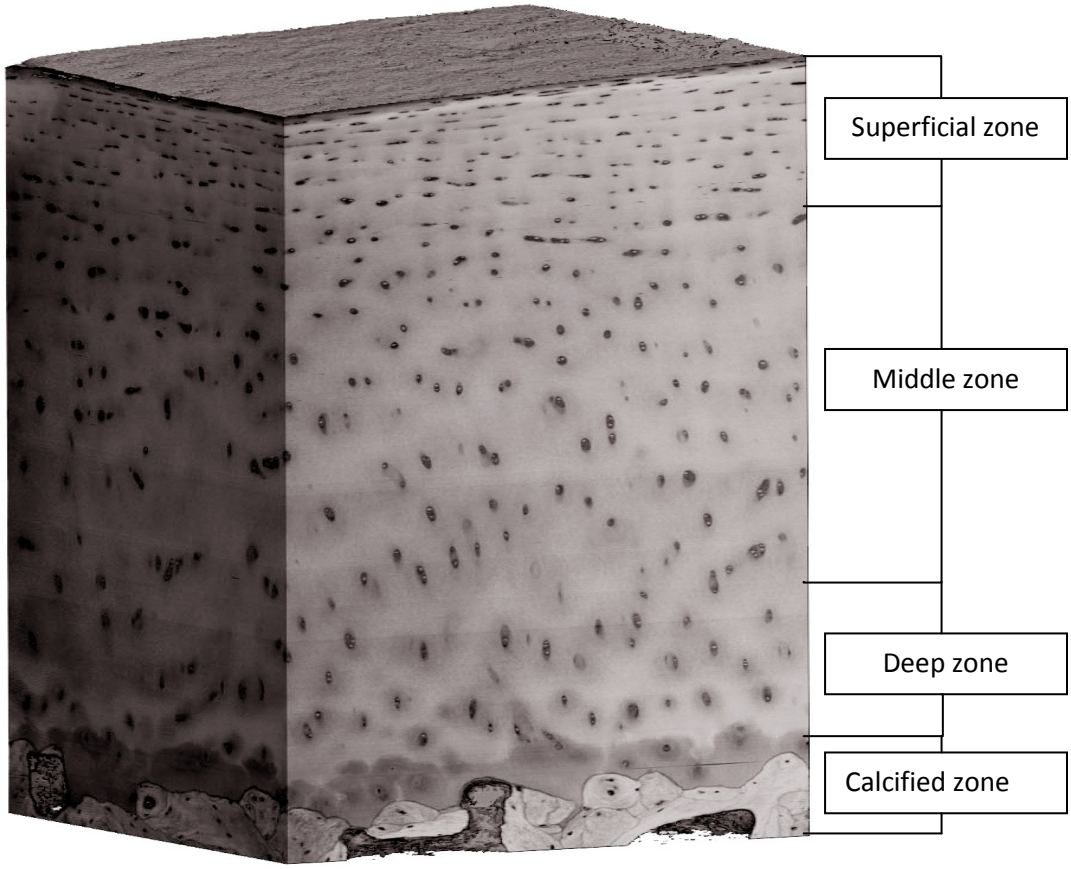

Figure 2.5: Chondrocytes are widely scattered in the matrix and their morphology varies according to their location. Image copied and adapted from (www.jacobsschool.ucsd.edu).

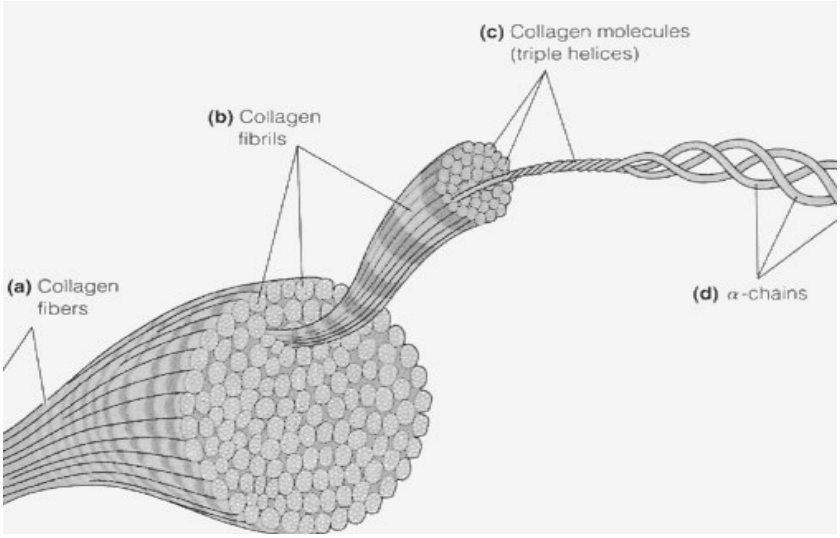

Figure 2.6: Collagen and its triple helix structure.

2.3.4. Collagen

Collagen is the most important protein in the animal body. It has a structural organisation which provides useful mechanical properties. There are 14 different kinds of collagen in human body. Among them type II collagen is important for articular cartilage. Approximately 65% of the matrix is collagen with some 80% of the collagen being type II, the remained types such as type VI, IX, X and XI (Martin et al., 1998). Collagen has a triple helix structure (Brodsky and Ramshaw, 1997) (Figure 2.6) which is responsible for the strength and flexibility of cartilage tissue.

Type II collagen helps maintain the structural integrity of the cartilage and plays a significant role in resisting indentations on the cartilage surface. Collagen type VI is scattered throughout the matrix and surrounds the chondrocytes which helps provide stabilization and anchorage for proteoglycans under stress (Hagiwara et al, 1992). Type XI collagen is a core of type II and controls the fibril growth of cartilage (Martin et al., 1998).

The extracellular matrix of articular cartilage contains large amount of type II collagen, which is important for the cartilage structure stability and the proper function of the articular cartilage. Type II collagen contains the greatest number of anti-inflammatory and joint supporting proteoglycans (Kuijer et al., 1988). Collagen provides tensile strength to the articular cartilage.

2.3.5. Proteoglycans

Proteoglycans are another structural component of cartilage which is found in the extra cellular matrix and on cell surfaces. Proteoglycans consist of a protein core of glycosaminoglycans which are covalently attached with Type II collagen (Rest and Maynell, 1987) (Figure 2.7). Around 25% of dry weight articular cartilage composed of proteoglycans. Chondrocytes manufacture proteoglycans and the water content and proteoglycan concentration vary in each zone of the tissue. At the articular cartilage surface the proteoglycan concentration is relatively low and the water content is high. In the calcified zone which is near subchondral bone the water content is lower and the proteoglycan concentration is higher (Mansour, 2003).

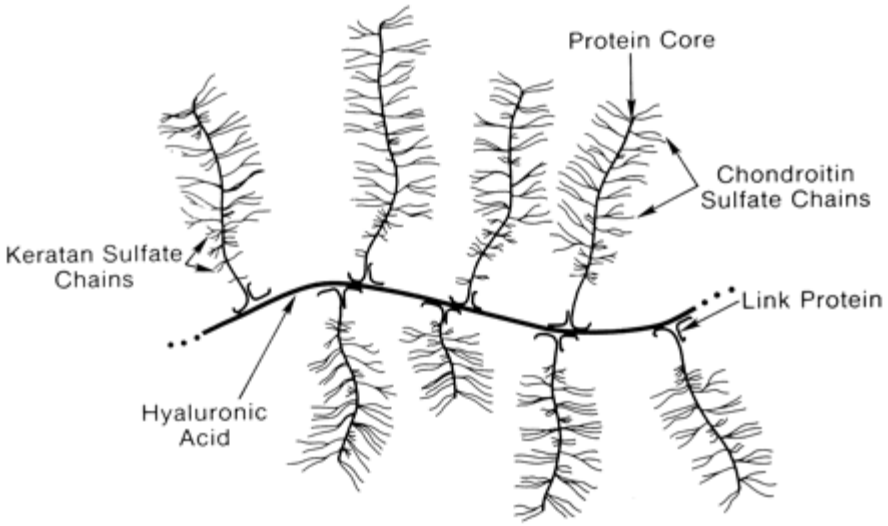

Figure 2.7: Proteoglycans, protein core and covalently attached structure.

2.3.6. Structural interactions of the components of cartilage

Due to the negatively charge proteoglycans, there is an osmotic pressure in the matrix which is as high as 1.7kgcm^{-2} (Maroudas., 1976). This osmotic pressure acts to hydrate the tissue which is balanced by a restraining elastic force due to the collagen fibre network. The net effect of these is termed the swelling pressure and it is based on the stiffness of its collagen-

proteoglycan matrix, the ion concentrations in the external fluid and its fixed charge density and distribution (Lai et al., 1991).

Cartilage degeneration is accompanied by the decrease in glycosaminoglycans in the tissue (Mankin and Lippiello, 1971; Maroudas et al., 1973). The cartilage is prevented from swelling to full extension by the collagen framework. The collagen fibres are in tension even when there is no external force applied to the cartilage because they constrain the osmotic pressure. When an external force is applied to the cartilage surface by an indenter, water in the cartilage will flow out from the tissue increasing the concentration of proteoglycans. Because of the higher concentration of proteoglycans the swelling pressure of the tissue will also increase until at equilibrium the swelling pressure is in equilibrium with the external force. The fluid movement when the cartilage is under load is controlled by the pressure difference of the internal and external stress and the tissue's permeability. The tissue permeability is based on the thickness of the tissue and density of the proteoglycans and collagen. The ability of the fluid to flow through the tissue therefore defines its time-dependent mechanical properties, i.e. its viscoelastic properties.

2.4. Mechanical properties of articular cartilage

Articular cartilage is porous and the extracellular matrix is filled with fluid. The mechanical properties of articular cartilage have either been characterized as elastic (Hayes et al., 1972), viscoelastic (Parsons and Black, 1977), biphasic (Mow et al., 1980) or triphasic (Lai et al., 1991). The mechanical properties of articular cartilage are based on its porous structure and its solid matrix. The cartilage consists of 75 to 80% of water and rest 20 to 25% only collagen and proteoglycan molecules (Figure 2.3). The cartilage mechanical properties are based on three important initial points.

Firstly, both the porous structure, with typical void dimensions of 50 Å (Martin et al., 1998), and the proteoglycan content determines the mechanical behaviour of cartilage. The solids content of cartilage, which comprises around 25% of the portion of the tissue, consists of collagen fibres and proteoglycan molecules. The remainder of the tissue is essentially water.

The proteoglycans attract water, so that the tissue is effectively swollen with water that is held in place by electrochemical interactions with the proteoglycans. The mechanical properties of cartilage will deteriorate if anything interferes with the proteoglycan content. The nature of chondrocytes is to produce new normal cartilage where it is damaged.

Secondly, the viscoelastic properties of cartilage also depend on its porous and water filled material. In particular, the cartilage elastic properties vary greatly with the rate of loading: at a very slow rate of loading the cartilage will withstand only few MPa, but under dynamic loading this may approach 500 MPa.

The mechanical properties of articular cartilage changes with the fluid movement when fluid moves in and out of the tissue under load and unload (Rohlmann and Reinhard Kölbel, 1987). The viscoelasticity of cartilage can be analysed by a simple indentation method in in-situ condition.

The test results are known in terms of the stretch ratio λ,

$$\lambda = \text{deformed gage length/initial gage length.}$$

Between human and animal, cartilage have significant differences in their biomechanical properties (Athanasiou et al., 1991). Mechanical properties of animal cartilage depend on the animal age, harvested place and testing method whether it is confined or unconfined compression (Ateshian and Hung, 2003). Young bovine articular cartilage cell density range is from 240–100 million cells per cm^3 through the depth of the tissue. The chondrocytes also play a significant role in biomechanical properties of cartilage (Jadin et al., 2003).

2.4.1. Fluid flow and biphasic theory

Under the action of fluid pressure gradients the cartilage fluid passes through the proteoglycan and collagen. The mechanical behaviour of cartilage based on collagen II fibre, proteoglycan gel and water (Jeffery et al., 1991). Physically, when articular cartilage is compressed the pressure gradient of the tissue is increased. As a result, the interstitial liquid begins to move within the tissue or is exuded from the cartilage (Lu and Mow, 2007). The biphasic model for cartilage considers cartilage as a combination of two interacting materials: a solid phase and liquid phase. This biphasic model is used to analyse the mechanical stress that is carried by

each component of the tissue. The biphasic model is used often nowadays to investigate the biomechanical properties of normal cartilage and repaired cartilage (Armstrong et al., 1982).

For fluid to flow within articular cartilage, it must be permeable which means how easy it is for the fluid to move in and out of the tissue. Articular cartilage permeability can be measured with the fluid flow ability through the solid phase of the cartilage such as extra cellular matrix and inversely proportional to the exuded fluid's friction drag. The fluid exudes from the specimen and it reduces both extra cellular matrix permeability and pore size when cartilage is compressed. As the result, fluid movement increases in the cartilage (Maroudas et al., 1968). This behaviour can be described in terms of creep and stress relaxation (Mow et al., 1980, Kempson et al., 1971). Creep is defined as the time-dependent mechanical behaviour of the material when it is subjected to a step-stress. During a creep response, a material will further deform with time following an initial deformation upon immediate application of the step-stress. With regards to articular cartilage,the tissue can't deform immediately, due to its fluid content and low permeability, but over time, the tissue will slowly compress, as fluid is exuded, until an equilibrium compressed deformation is attained.

By contrast, stress relaxation is defined as a material's stress response to a step-strain. When stress relaxation occurs, the stress needed to maintain a constant total deformation decreases as a function of time.

Macroscopically, cartilage is well described by Darcy's law (Darcy 1856) which states that the rate of volume fluid discharge through a porous solid is related to the pressure gradient applied to the solid and the hydraulic permeability coefficient k. Mathematically, Darcy's law is stated as follows:

$$Q = kA\Delta P/h$$

Where A is the area of the specimen, ΔP is the pressure gradient, h is the thickness, and k is the hydraulic permeability coefficient (Kovach., 1996).

2.4.2. Indentation properties of articular cartilage

Short duration indention testing on the cartilage has proved that as a potential method for assessing the quality and function of articular cartilage. The indentation testing is non-destructive, quick and quantitative assessment for analysing the biomechanical properties and

function of articular cartilage which has been used in a number of studies (Kempson et al., 1971; Lyyra et al., 1995). Recently arthroscopic probes used for short duration indentation protocols have been developed for testing the human articular cartilage (Lyyra et al., 1995; Niederauer et al., 1998).

Generally, a rigid metal tool with plane head or spherical head indenter used to indent the soft tissue surface and force-displacement characteristics recorded (Al-jaafreh et al., 2008). The general acceptance of indentation test carried out so far is that cartilage is viscoelastic material. The articular cartilage creep and relaxation properties have been compared only in few studies. According to Van Mow, recovery was slower than the creep deformation (Mow et al., 1980). On the other hand stress relaxation takes place more quickly than creep deformation (Li et al., 2008).

2.4.3. Bovine vs. Human cartilage

Many studies have been carried out with bovine articular cartilage (Ateshian., 1997, Vunjak-Novakovic et al., 1999, Demarteau et al., 2006) and human articular cartilage (Armstrong et al., 1982, Basser et al., 1998, Demarteau et al., 2006). Demarteau et al., (2006) are one of the few researchers to directly compare human and bovine articular cartilage using the same methodology. They found that, at 10% compression, human cartilage was stiffer and less permeable than bovine cartilage: the confined compression modulus was 2.22 ±0.65 MPa for human femoral head cartilage, compared to 0.57 ± 0.27 MPa for bovine humeral heads and hydraulic permeabilities were 1.1 ± 0.6 x 10^{-15} m^4/Ns and 2.3 ± 1.2 x 10^{-15} m^4/Ns respectively. Furthermore, Young's moduli were 1.64 ± 0.34 MPa and 0.28 ± 0.14 for human and bovine cartalige, whereas Poisson's ratios, however, did not differ between the species at 0.14 ± 0.09 (Demarteau et al., 2006).

2.5. Mechanical Testing methods for Articular Cartilage

2.5.1 Introduction

Compression is the obvious way in which to mechanically test articular cartilage. There are three basic commonly accepted types of test in use for the determination of the mechanical

properties of articular cartilage: confined compression, unconfined compression and indentation.

Confined compression method is a widely used technique (Schinag, 1997, Chen, 1997) where the osteochondral plug is mounted in a confining holder, surrounded by physiological solution, and which resists radial expansion and fluid leakage and only allows uniaxial deformation of the cartilage (Kwan et al., 1989). A porous indenter is applied to the cartilage surface which then compresses with time as the fluid is expelled from the sample back through the indenter. The unconfined compression test is another commonly used technique in cartilage biomechanics and cartilage tissue engineering (Mow et al., 2002). The unconfined compression method has been frequently used for investigating biomechanical properties of cartilage (Armstrong et al., 1984, Sah et al., 1989). It is similar to the confined compression technique, except for fluid and solid is allowed to move laterally under an axial load.

It should be noted that confined compression and unconfined compression are the two extreme conditions that bound the physiological condition. A more physiological response to load may be determined using an indentation test.

2.5.2. Indentation of articular cartilage

The indentation test (Figure 2.8) is often used for evaluating the cartilage, whereby a stress is applied to the cartilage surface using the small indenter and the results (creep and relaxation) are observed during the indentation time. The indenter head may be flat or spherical or impermeable (Li and Herzog, 2005).

Both elasticity and viscoelasticity can be analysed by the indentation method (Korhonen et al., 2002) both in vivo and in vitro. The indentation method is an efficient and it can be used to evaluate the same specimen in different sites non- destructively (Smith and Mansour, 2000, Perie et al., 2005, Franz et al., 2000, Duda et al., 2004). The indentation test has stimulated theoretical modelling which involves a basic understanding of the contact problem with an elastic medium. Boussinesq's problem explains the determination of stress and displacement in an elastic half-space indenter by the rigid indenter is known as the famous Boussinesq problem (Boussinesq, 1885 cited by Sakamoto et al., 1996). If the indentation method works properly, the characterization of the biological tissues mechanical properties will be the simple task (Sakamoto et al., 1996). There are many types of indentation testing methods in use such as

arthroscopic indentation and static indentation which are classified into mainly two types: in vitro and in vivo. Indentation tests on cartilage are commonly performed in vitro. The in vitro indentation tests are carried out within a few hours post-mortem degeneration, of cartilage which would not damage the cartilage properties (Kiefer et al., 1989).

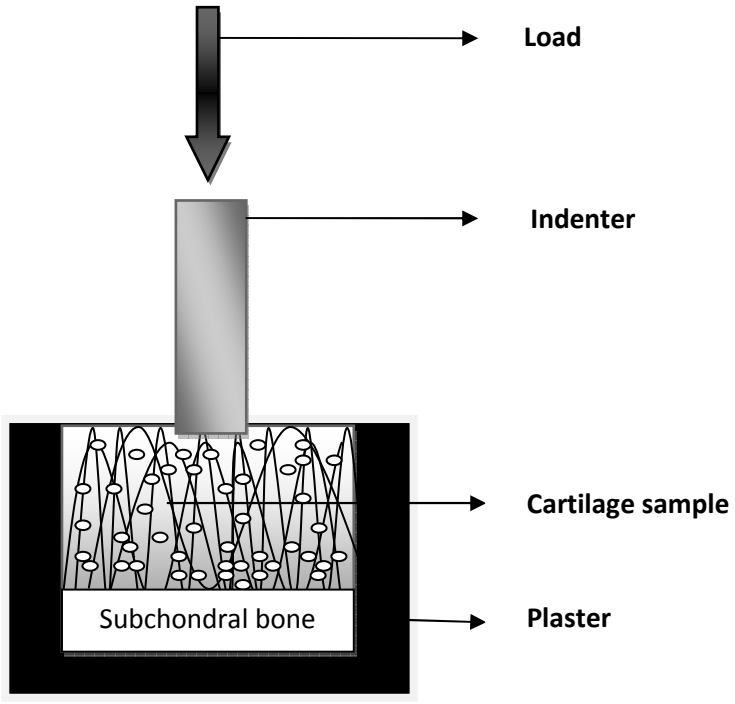

Figure 2.8: During indentation method, the sample (cartilage) is compressed with an indenter.

2.5.3. Arthroscopic indentation instruments

A number of arthroscopic indentation instruments already exist on the market (e.g. Artscan 200, Artscan Oy, Helsinki, Finland; Arthro-BST, Biomomentum, Laval, Canada). However, these handheld devices are not suitable for evaluating the articular cartilage stiffness primarily due to slipping of the indenter on the surface of the articular cartilage (Toyras et al., 2005). Furthermore, these devices only measure a stiffness parameter, and the viscoelastic properties of the tissue are ignored. Finally, these devices do not allow the applied force on the surface to be varied based on the thickness of the cartilage and place; the applied force is an important parameter, because, applied force is directly related to the deformation.

Robotic or haptic orthopaedic surgery (e.g. MAKOplasty, MAKOsurgical Corp, Ft Lauderdale, USA) offers a potential alternative to hand held devices whereby the indentation system can be located on the end of a mechanical arm. The precise location of the indenter and hence degenerate tissue will be known by the registration process of the computer aided orthopaedic device. The physician or robot can track the mechanical arm over the surface of the cartilage to investigate its condition. It may therefore be suggested that using a mechanical arm will overcome the hand held cartilage testing device problems.

2.5.4. Types of indenter

There are typically two types of indenter used on articular cartilage: a plane (flat) ended indenter, and an indenter with a hemisphere as it tip (spherical indenter).

A spherical indentation tool produces comparatively uniform deformation even at the edge of the contact region of cartilage. The spherical head indenter does not make any physical damage to the surface of the cartilage, however it can slip easily on the articular cartilage surface due to the lubricated, smooth surface (Li and Herzog, 2006). Whereas a flat ended indenter tip does not slip as easily from the cartilage surface.

The stress environment created by each tip is different due to their geometries. A spherical indenter produces stress concentrations in the centre of the indenter, whilst the flat-ended indenter produces stress concentrations at its edge. The chondrocyte death rate during indentation is much higher with the spherical indenter than the flat-ended indenter due to the deep compression and larger strain closer to centre of the indenter (Bae et al., 2007). Nonetheless, the flat-ended indenter does cause cell death, which begins around the contact region as like a ring shaped area on the cartilage surface (Bae et al., 2007).

2.5.6. Preconditioning of cartilage

The purpose of the preconditioning study is to evaluate the in vitro load and relaxation behaviour of the cartilage when doing cyclic loading on cartilage (Kunkel et al., 2007). Preconditioning puts the sample into a state where repeated tests output the same results, which

can then be considered indicative of the true behaviour of cartilage. Preconditioning of articular cartilage with a constant load (0.03–0.05 N) was applied prior to apply the actual test load. The actual load for human and bovine samples is 0.19 N. The test load was loaded on the cartilage surface suddenly and the specimen is allowed to deform. The precondition was calculated when there is no value further after in 20 minutes which takes 3000 seconds (Athanasiou et al., 1991). The specimen was tested using the confined compression technique. However, it is not known, to the author's knowledge, whether there is a preconditioning effect with regards to indentation testing: are multiple tests performed at the same position on the surface mechanically equivalent? If they are one may conclude that the cartilage is preconditioned. Once preconditioned, another question is: how long will it take to return to the original mechanical behaviour of the preconditioned state?

2.5.7. Recovery test of cartilage

The purpose of the preconditioned cartilage recovery experiment is to evaluate how long it takes for the cartilage to recover to the pre-test condition. This will provide information regarding the viscoelastic recovery of the cartilage, an important parameter if the cartilage is to be repeat-tested.

The biomechanical properties of articular cartilage are a function of the water content of the tissue, which is predominantly maintained by hydrophilic glycosaminoglycans (Urban et al., 1979). The equilibrium position will be controlled by the mechanical behaviour of the solid phase. When cartilage surface is indented, the crimped collagens fibres, aligned parallel to the surface of the cartilage, straighten. Once straight, their stiffness increases, since continued deformation requires a lengthening of the fibre itself. During cartilage recovery the fibres will restore to their original position and, as with all cartilage mechanics, the flow of fluid through the tissue will control the time-dependent properties of the tissue (Eckstein et al., 1999).

2.6. Research objectives

The above literature review has highlighted an area of research that may be of benefit to both surgeon and patient in the treatment of osteoarthritis. Therefore, this thesis has the following objectives, reiterated from section 1.2:

1. To design, build and evaluate a bench top indentation system to assess the viscoelastic properties of articular cartilage, which has the potential to be converted to a device that could be used arthroscopically and intraopertively.

And using the above indentation system:

2. To investigate the difference between a spherically headed indenter and a flat headed indenter in assessing the cartilage mechanical properties in vitro.
3. To evaluate the cartilage's preconditioning properties by cyclic indentation testing.
4. And to evaluate the recovery of articular cartilage subsequent to the preconditioning.

3. Machine construction

3.1. Introduction and rationale

Before an indentation system can be mounted on a robotic arm, validation tests should be made in a simpler environment. To this extent it was necessary to design a bench top indentation system, capable of performing high resolution indentation tests on articular cartilage samples.

After design meetings, it was decided to use a spring based linear variable displacement transducer (LVDT) to both apply a force and determine a subsequent displacement. To apply the load, it was decided to mount the LVDT on a high resolution linear actuator, which would drive the LVDT into the surface of the cartilage. Whilst the load would be proportional to the deformation, making analysis more difficult than with constant stress or strain devices, it was felt that this probe was an ideal shape to be used arthroscopically.

3.2. Bench top frame

The bench top materials testing machine (MTS) was designed in Pro|Engineer, which is a 3D computer aided designing tool by Parametric Technology Corporation (PTC), USA. The machine was fabricated in-house, in the Bioengineering Unit's mechanical workshop. The MTS consists of 6 parts, all made from aluminium. The part names are as follows:

- Machine Base
- Tissue placing plate
- Right support
- Left support
- Top plate for fixing actuator
- Lab jack

3.2.1. Base plate

The base section is an important section for the machine (Appendix, Figure 10.1). The base was designed to be rigid providing a solid foundation for the vertical supports. The base plate was fitted with rubber feet in each corner to reduce bench vibrations. The base plate has 2 square cavities for fixing the left and right side supports.

3.2.2. Left and Right side supports

The total height of both supports is 40 cm and both supports are fixed perpendicular to the base plate (Appendix, Figure 10.2 and 10.3). The tissue holding plate is fixed between these two supports using a 5x5x250 mm (width x depth x height) cut and screws for moving the tissue holding plate up and down using the lap jack. The top plate is fixed at the top of the two supports.

3.2.3. Tissue holding plate

The tissue holding plate is a simple plate having two notches for fixing in the supports (Appendix, Figure 10.4). The tissue holding plate is placed in between the two supports and parallel to the base plate. The tissue holding and base plate are connected via a lab jack. The lab jack is used for adjusting the height of tissue holding plate. A grooved sliding mechanism is used to move the tissue holding plate up and down with reference to the supports. The tissue placing plate is fixed tightly in place using screws which fix to the other sides of the supports.

3.2.4. Top plate

The top plate is like as inverted 'T' shape (Appendix, Figure 10.5) fixed in between both supports at the top of the supports. The linear actuator is fixed in the middle of this plate using screws. The top plate is attached perpendicularly to both supports.

3.2.5. Lab jack

The lab jack provides complete stability in any position and height adjustable support between base plate and tissue holding plate also smooth and continuous operation for full range extension and shrink. Easily set the exact height needed with the turn of the knob.

3.3. Machine electronics parts and function

3.3.1. Linear Actuator

The actuator (Model no RSSA20-24, Kumina-20 series, Sebong Techno Co., Ltd, Japan) was supplied by Reliance Precision Mechatronics, Huddersfield, England. It has a stroke length of 20mm and position repeatability of ±0.005 mm (manufacturer's figure) (Figure 3.1). The smooth up and down movement is controlled by a 5 phase stepper motor. The reliance actuator is slim and very high accuracy which helps for accurate depth indentation on cartilage surface.

The stepper motor is controlled by the micro step driver board according to the input signal comes from computer. The driver program was developed in the Matlab environment by Dr Philip Riches (Appendix) and the actuator stepper motor rotation speed, rotating direction, start and stop is controlled from computer through the driver board.

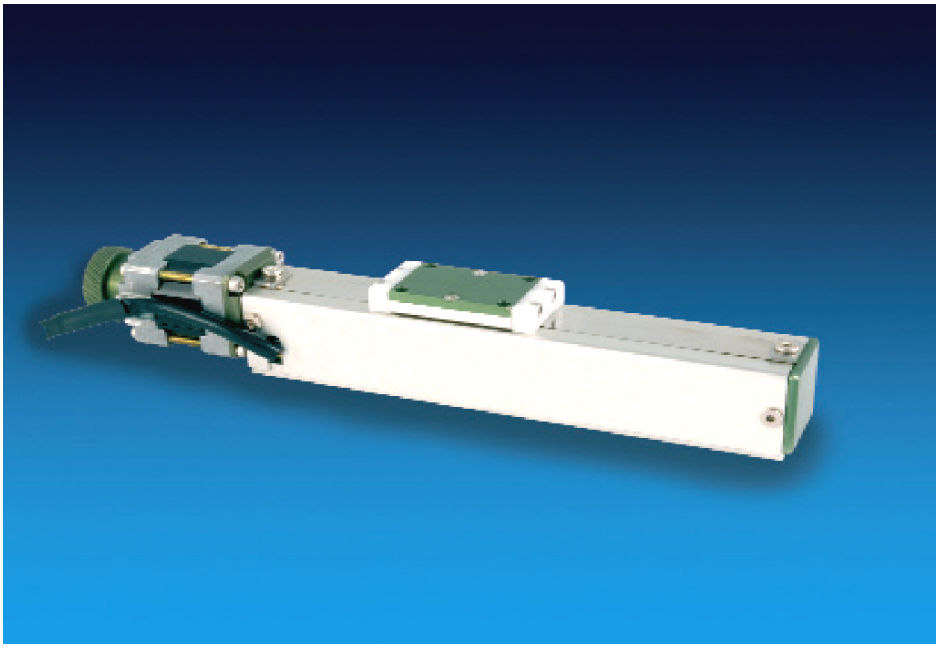

Figure 3.1: Photograph of the actuator. Courtesy of RP Mechatronics (http://www.rpmechatronics.co.uk/products/miniature-actuators.html).

3.3.2. LVDT displacement sensor

The spring loaded LVDT (Linear Variable Differential Transformer) displacement sensor (Max displacement – 10mm, SangamoTransducers, 52457) was used for both applying the load and measuring the creep properties during indentation on cartilage surface. The output of the LVDT varied between -10 to +10 V depending on the deformation of the LVDT. A material testing machine (Instron 5800R) was used with a 10N load cell to apply a known displacement (x) and to measure the force (F) in the spring of the LVDT in order to calculate the spring constant (k), where $F = kx$. A typical force displacement curve is provided in Figure 3.2. The average

gradient of the linear region of the curve, which is equal to the spring constant *k*, was equal to 0.131N/mm

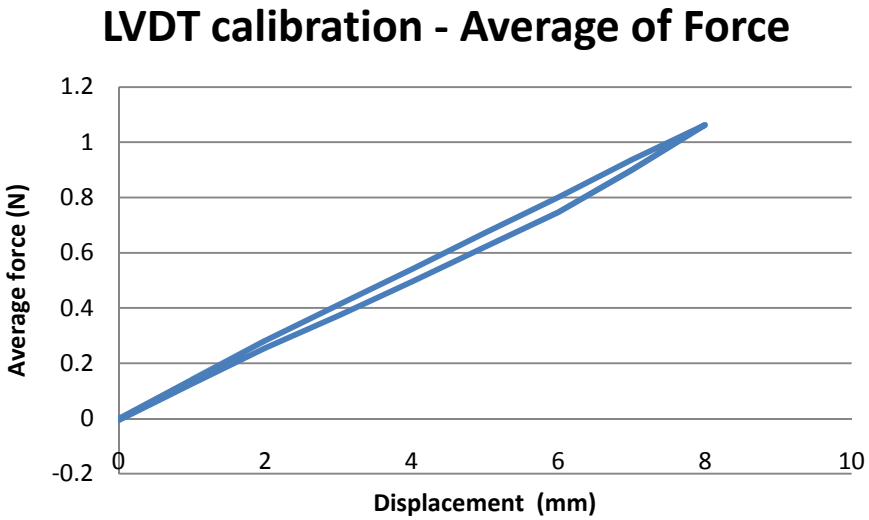

Figure 3.2: Force-displacement characteristics of the LVDT. The spring stiffness is calculated with reference of machine force sensor.

Figure 3.2 shows evidence of minor hysteresis, and possible non-linearity in the relationship between force and extension. However, for the purposes of this thesis, these errors in the measurement of force were discounted and not quantified. Clearly, if the indentation device was improved upon, it would be desirable for such effects to be minimised. The main advantages of the LVDT displacement sensor is that, once calibrated, it offers both force measuring capability and displacement measuring capability in a device shaped appropriately for arthroscopic insertion. In addition to the spring constant being determined, the calibration between displacement and LVDT output voltage is also required, and this formed part of the experimental experimental protocol the results of which are described in Figure 4.2.

3.3.3. Data acquisition unit

The main purpose of the data acquisition module (Model no – DI148U, Dataq instruments Inc, Ohio, USA) (Figure 3.3) is to convert analog voltage into digital signals with 10 bit resolution in successive approximation method. The corresponding signal was converted into mm with help of a Matlab driver program, written by Philip Riches, and stored on the hard disk. The maximum input voltage level is ±10 volts which is compatible with our sensor signal

conditioner and the sampling frequency of the DAQ was 60 Hz. The DAQ is a compact size and derive the power source through communication cable from the host computer, thus eliminating the external power source. The data from the DAQ was retrieved through a Matlab program and stored on the hard disk.

Figure 3.3: Dataq data acquisition instrument. Copied from (http://www.dataq.com/products/startkit/di148.htm).

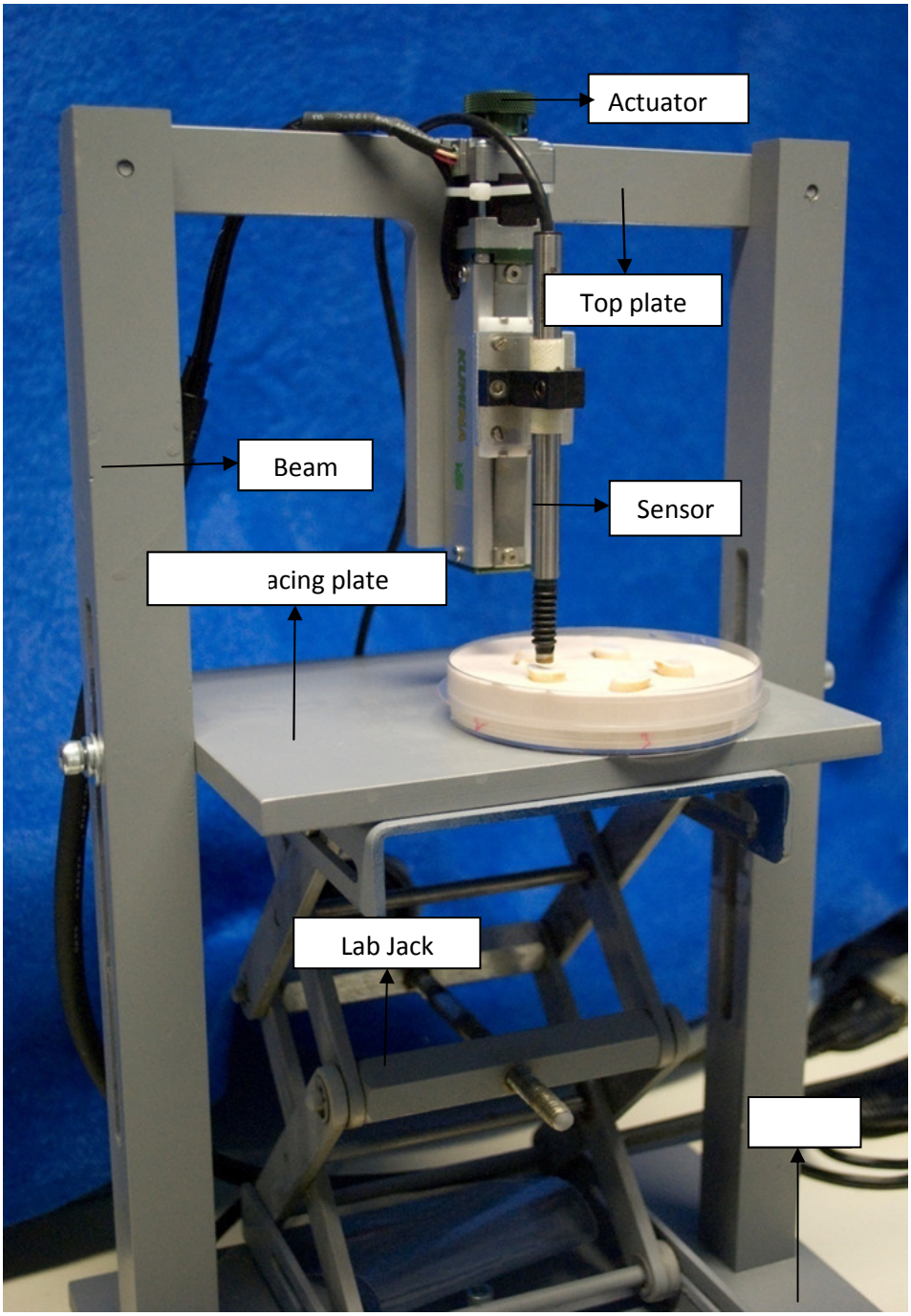

Figure 3.4: The original image of the material testing machine.

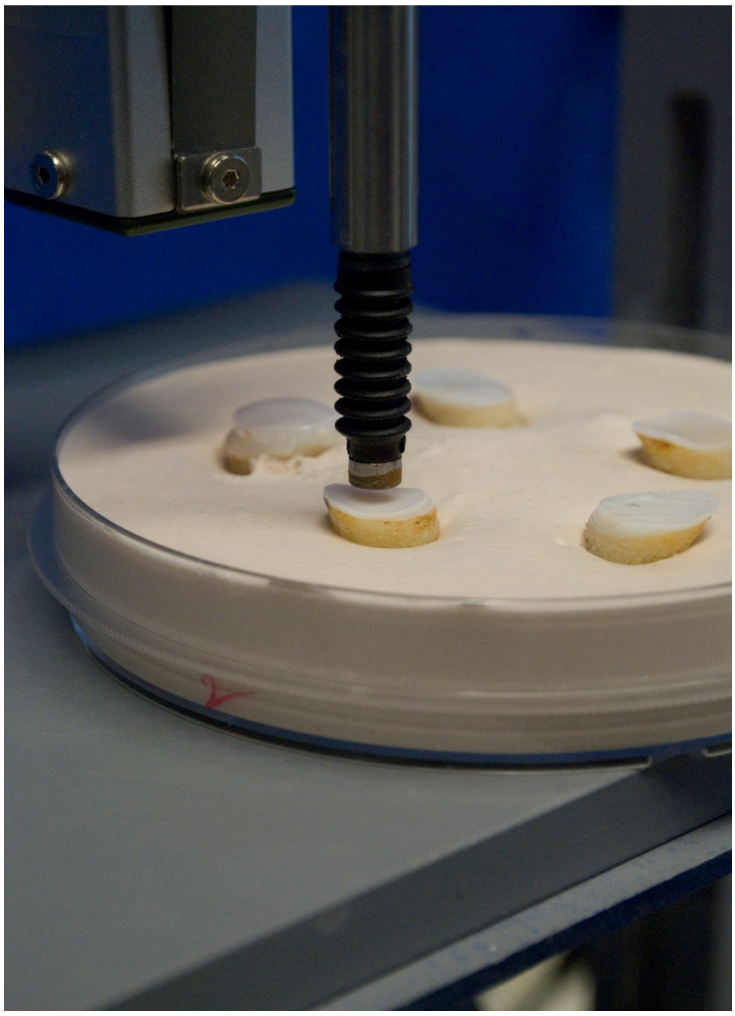

Figure 3.5: The plugs are placed directly under the sensor tip for measuring the creep properties of the cartilage.

3.4. Machine working principle

The bench top MTS (Figure 3.4) machine's actuator movement and displacement sensor data actuation is controlled from the computer using a Matlab program. Before testing the cartilage, the sensor is calibrated by doing an indentation on a metal plate. Because the metal frame is a

relatively stiff it is assumed that its deformation is negligible. The LVDT, via its integral spring produces the indentation force on the surface and measures the surface deformation. If there is no deformation, the sensor displacement is equal to the actuator displacement. After placing the osteochondral plug contained in the petri dish right under the sensor head (Figure 3.5), the distance between sensor head and tissue surface is adjusted with fine tuning of turning of the jack knob. Then a control signal is sent to the actuator driver board to operate the actuator stepper motor. Simultaneously the sensor signals are collected through the signal amplifier and data acquisition unit and recorded on the hard drive for further analysis.

4. Programming method and control

4.1. Introduction

A dedicated computer program was written to interface with the indentation system. The program was written in Matlab (The Math Works, US) and the code is presented in Appendix (10.2). The actuator stepper motor rotation speed and direction is controlled from the computer COM port. The actuator movement is controlled by a 5-phase stepper motor which delivers high resolution (2500 pulse=1mm displacement) on the order of one degree per step. The cartilage deformation data is collected from the LVDT displacement sensor also via the same program. The software flow chart is shown in the Figure 4.1.

4.2. Flow chart

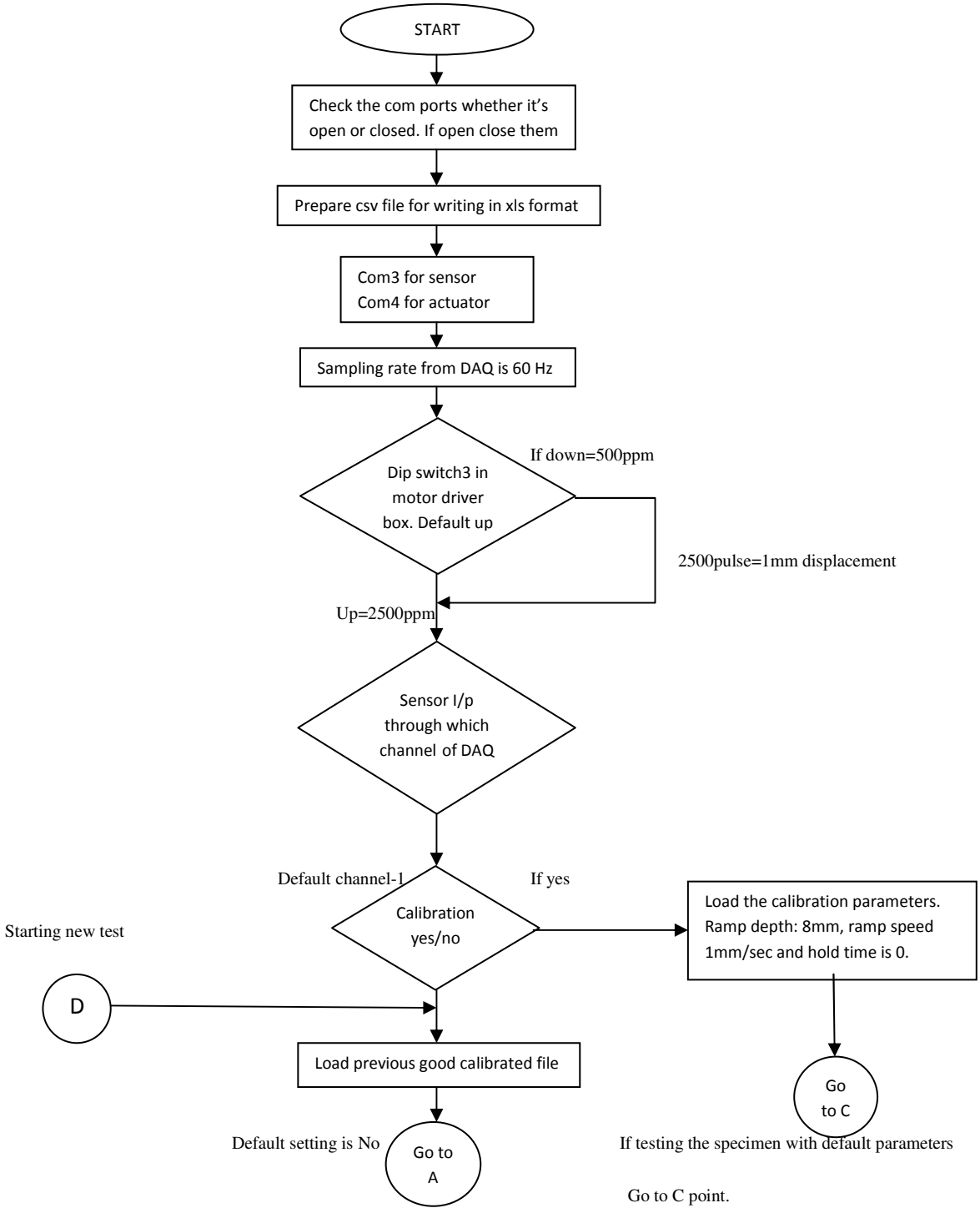

Figure 4.1 (part 1): Continued page no 35-36.

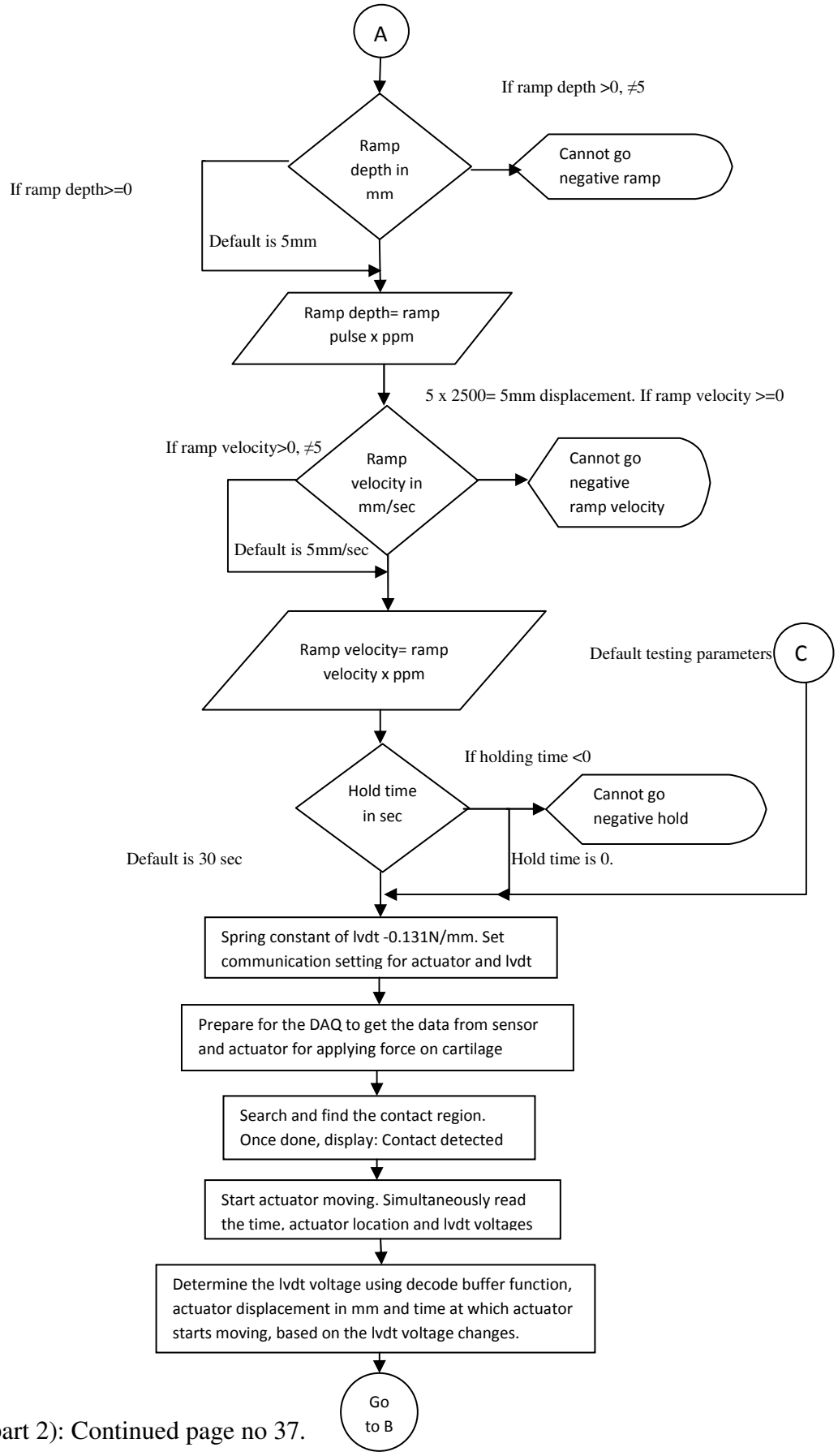

Figure 4.1 (part 2): Continued page no 37.

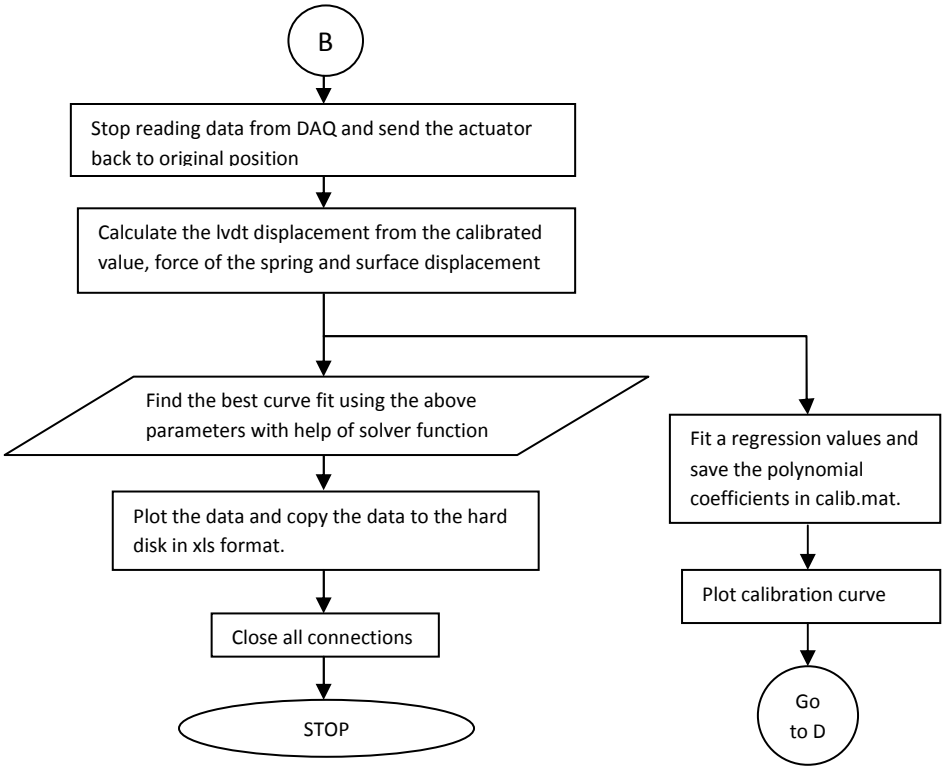

Figure 4.1(part 3): The software flow chart and its working procedure.

4.3. Working principle

4.3.1. Calibration

The calibration test equates the actuator displacement with lvdt sensor displacement while indenting on a metal surface to convert the voltage output of the LVDT into displacement. The calibration process was done before each tissue sample was tested. The calibration parameters were the same every time, which were an 8mm ramp depth, 1mm/sec ramp speed and zero holding duration. After gathering all the data from sensor and the actuator, the calibration program plots the diagram of sensor volts against actuator displacement (Figure 4.2). Despite the calibration curve being close to a straight line, a second degree polynomial function was used for fitting the curve here.

$$y = a_2 t^2 + a_1 t + a_0$$

To find the unknown coefficients a0, a1 and a2 the following Matlab function was used.

p = polyfit (sensor volts, actuator location, 2).

The above function finds the 2nd degree of the p (sensor volts), and that fits the data p (sensor volts (i)) to p (actuator location (i)) in the least square sense. i.e. it converts a voltage into displacement. Matlab calculates the polynomial coefficients in descending powers and stores the p values in memory for the next test. For example:

p = 0.1823 0.2534 0.6325.

The second-degree polynomial model of the data is given by the following equation:

$$y = 0.1823t^2 + 0.2534t + 0.6325$$

One can then evaluate the polynomial with the sensor voltage:

Curve fitting = Polyval (p, sensor volts).

Plolyval function returns the predicted value of a polynomial given its coefficients, p, at the values in sensor volts.

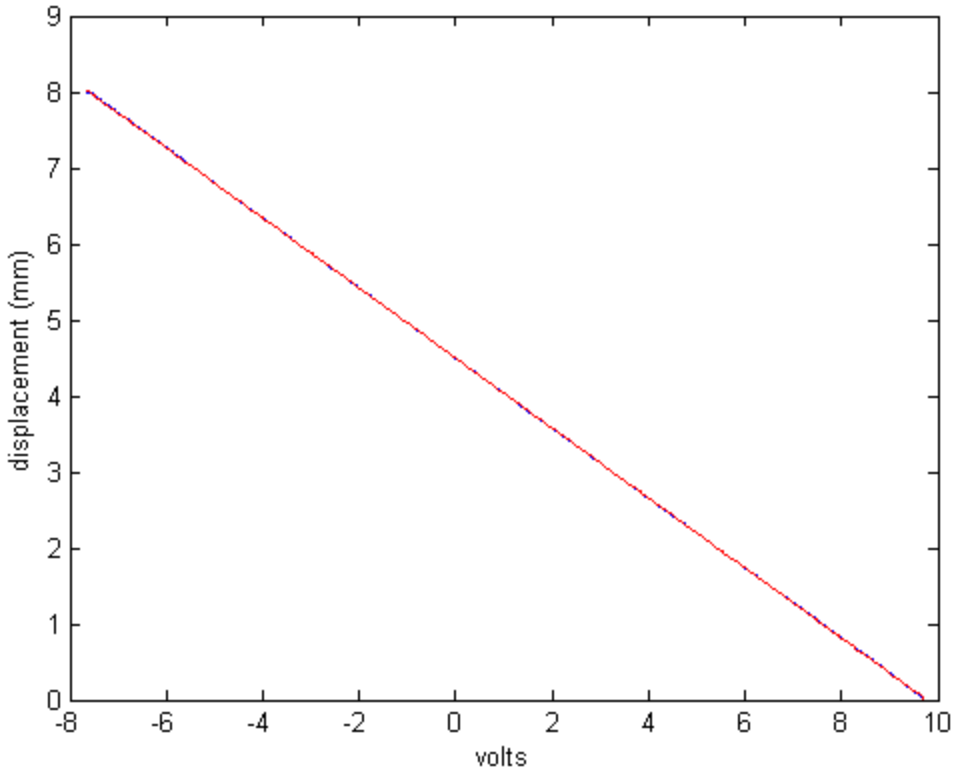

Figure 4.2: Typical calibration curve showing relationship between linear actuator displacement and LVDT voltage on a very hard surface. This enables calibration of the LVDT converting a voltage into a known displacement of the spring.

4.3.2. Osteochondral plug testing procedure

All the samples were tested with the same parameters which were an actuator ramp depth 5mm and speed of 5mm/s with a holding duration of 30 seconds. The program loads the relative position ramp data to the actuator driver board and simultaneously monitors the lvdt displacement sensor voltage level. If there is any change in sensor voltage level, which confirms the sensor head (indenter) reached the cartilage surface. The program then displays the following message “contact detected”. After that program immediately loads the 5mm ramp

data to the actuator driver section and collects the data from sensor with respect to time. After 30 seconds the program sends a command to the driver board to return the actuator back to original position (home).

After contact, the next procedure is the calculation of surface displacement. The surface displacement if cartilage is calculated by using the following equation.

Surface displacement = Actuator displacement – LVDT sensor displacement.

Three plots are created (Figure 4.3). First one is displacement against time of cartilage (Green) with curve fitting diagram using polynomial function (Blue). The middle one is lvdt sensor displacement against time. The last one is force against time. Finally, the data are stored on the hard drive in Excel format. The last step of the program is close all the ports and ready for next test.

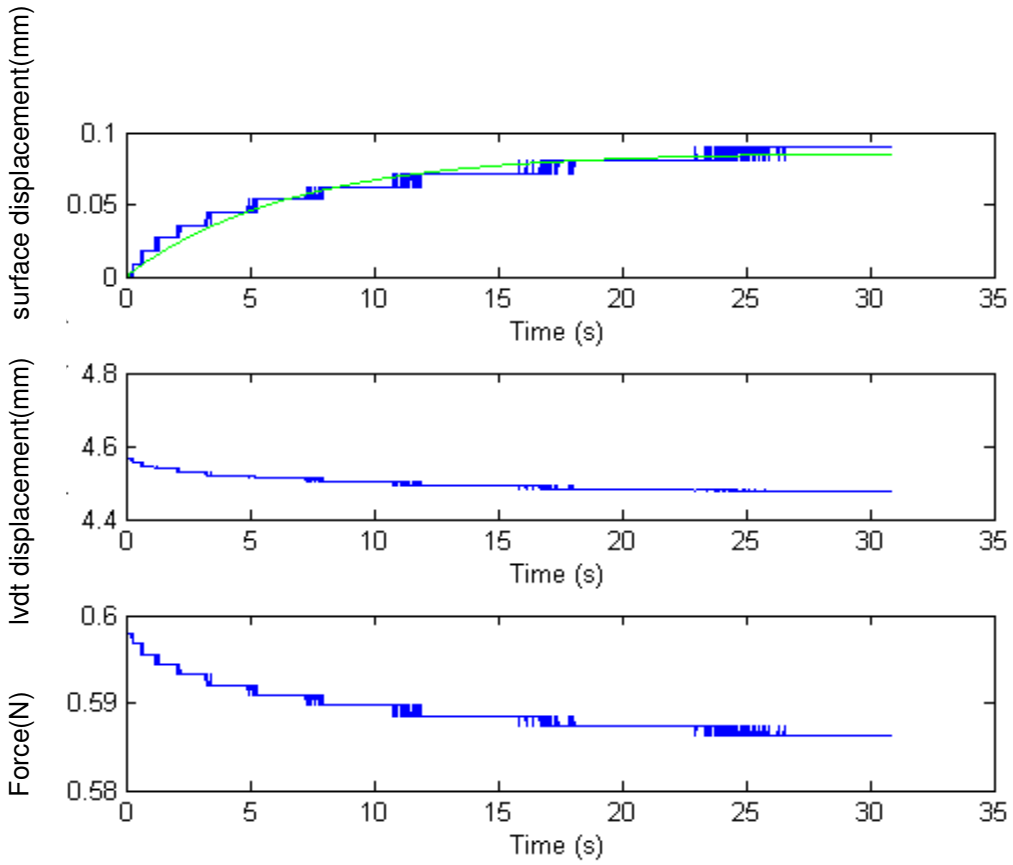

Figure 4.3: The typical output of indentation on the cartilage surface and displacement recorded once contact with the surface had been established (blue lines indicate experimental measures, green line is best fit according to equation 1). Time = 0 indicates time of contact.

4.3.3. Calculation and data analysis method

After finishing the test, Matlab generates the set of data and stored in hard drive in Excel format which contains time (t), Actuator displacement, LVDT displacement and surface displacement. After finishing the test the asymptote (A), slope (B) and displacement (d) were calculated by using the following equation and excel solver function.

$$d = A(1 - exp^{-Bt}) \qquad \text{Eq. 1}$$

Clearly, if t = 0, d = 0, and if t = ∞, d = A.

This function was chosen because it was the simplest function that fitted the data reasonably well. After collecting the data, the slope (*B*) and asymptote (*A*) were calculated in Excel sheet using the solver function, minimising the sum of the square of the differences between the data and the equation. The following diagram (Figure 4.4) was plotted in Excel spread sheet with the values generated by program during indentation (surface displacement of cartilage – steps curve) test and generated by Excel spread sheet (linear curve) while calculating the values of slope and asymptote. The following diagram (Figure 4.4) used to verify the accuracy of values of slope and asymptote. The spherical head and plane head produced deformation on the cartilage surface was calculated and compared with one another using T tests. The T test was also used for comparing the deformation difference between indentation on a metal plug and indentation on the cartilage.

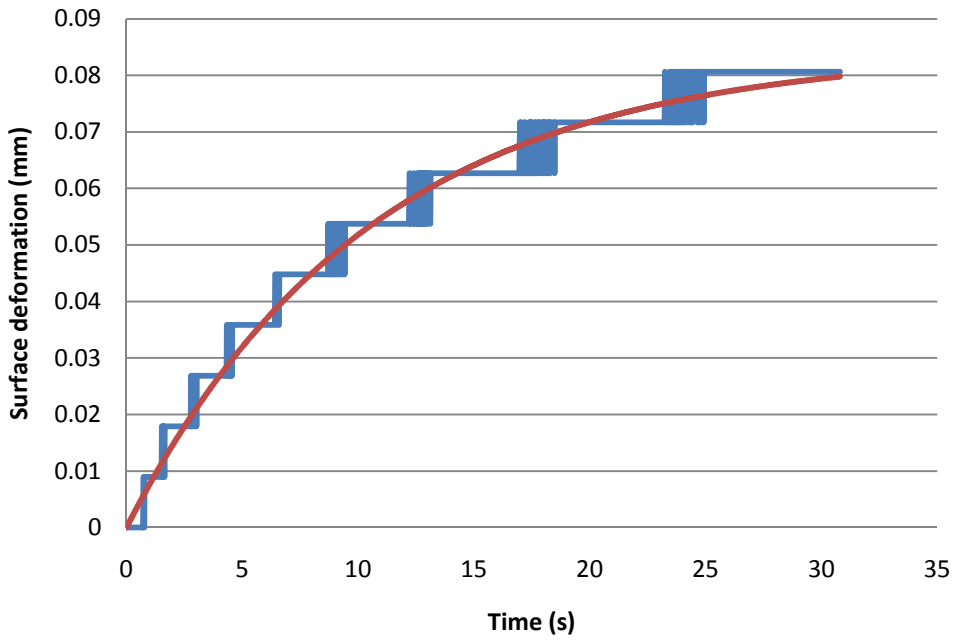

Figure 4.4: Typical example of surface deformation during the indentation test on the cartilage.

5. Tissue preparation

5.1. The bovine tibial plateau articulating surface

Bovine articular cartilage is frequently used for confined indentation testing (Julkunen et al., 2008; Korhonen et al., 2002; Ateshian., 1997; Appelman., 2009; Kieferet et al., 1989). The bovine knee joint articulating surface (Figure 5.1) is almost double the size of the human knee joint and many more osteochondral plugs can be harvested from a single knee. Approximately 10 plugs (each 10 mm in diameter) can be obtained from each tibia. In total 51 osteochondral plugs were used: 8 plugs for evaluating the spherical head indenter, 8 plugs for plane-ended indenter assessment, 10 plugs in the preconditioning experiments, and 25 osteochondral plugs to evaluate the recovery properties of the cartilage.

5.2. Tissue preparation procedure

Fresh bovine knee joints were obtained from a local butcher's shop. The surrounding soft tissues (e.g. meniscus and ligaments) of the joint were removed using a scalpel (Figure 5.1). Using a band saw, a cut was made perpendicular to the bone axis, through the subchondral bone. This resulted in a separation of the medial and lateral condyles (Figure 5.2). Cylindrical osteochondral plugs were taken from the tibial plateau using 10 mm hole punching tool (Figure 5.3 and 5.4). The plugs total size was around 1cm with the bone size of 0.8 cm and cartilage size was >2 cm (Figure 5.4). Preparing a perfect cylindrical plug with flat surface is impossible (Mow et al., 1980). After harvesting, the plugs were put in physiological solution (PBS). Plaster of Paris was prepared in a petri dish and the plugs were placed in it (Figure 5.5). The total depth of plaster of Paris was around 1.3 cm. The depth of the plaster below the sample was around 4 cm. Then the petri dish was covered with physiological solution and kept in the freezer. Cartilage is often frozen for long term storage. Cartilage freezing and thawing does not make difference to the mechanical behaviour of articular cartilage and cryopreservation is a suitable method for maintaining the cartilage mechanical behaviour (Kiefer et al., 1989). All the cartilage joints and osteochondral plugs were treated the same way. Prior to testing the petri dish was removed from freezer, then the sample was allowed to thaw at room temperature for a minimum of 3 hours.

Figure 5.1: Bovine tibial plateau.

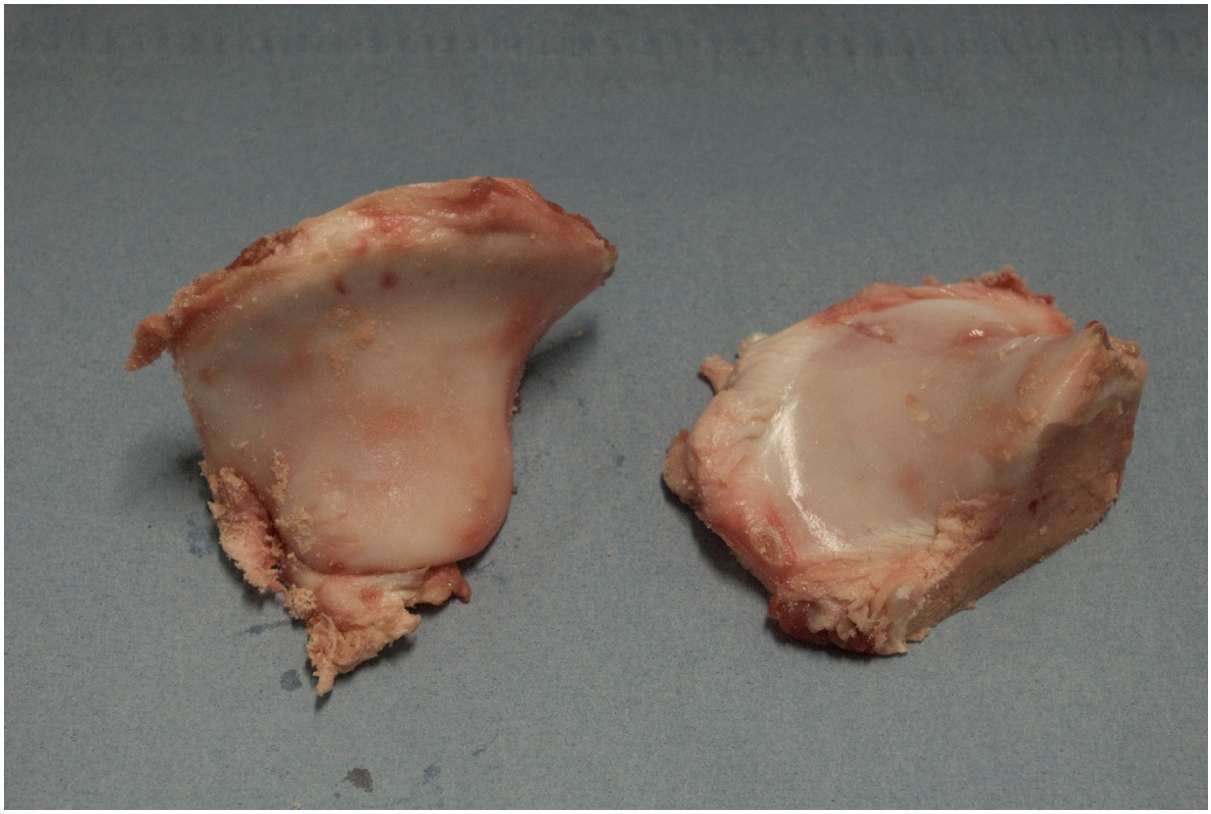

Figure 5.2: The joint surfaces which were obtained from the plateau.

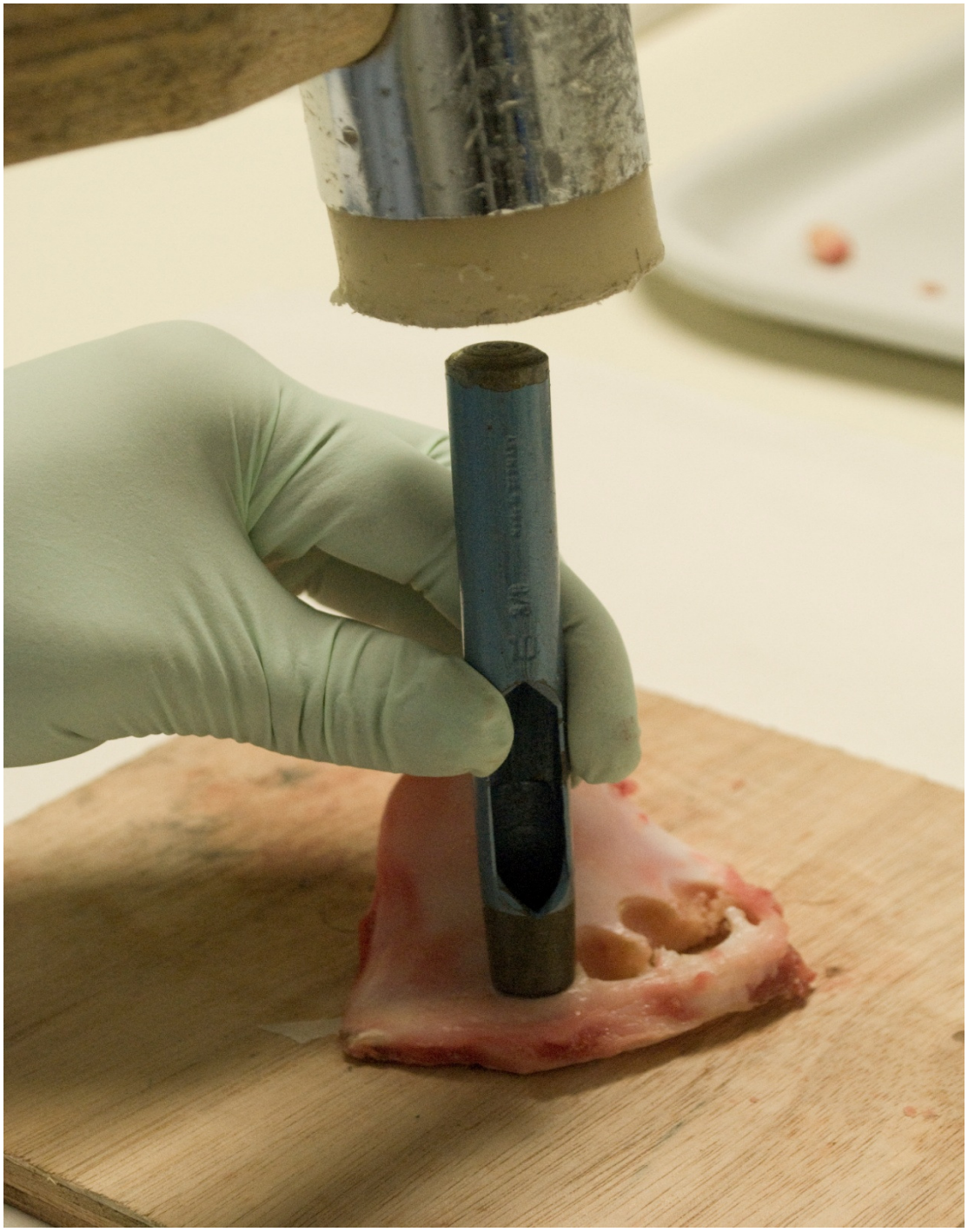

Figure 5.3: The osteochondral plugs were prepared from the joint surface using 10mm punching tool.

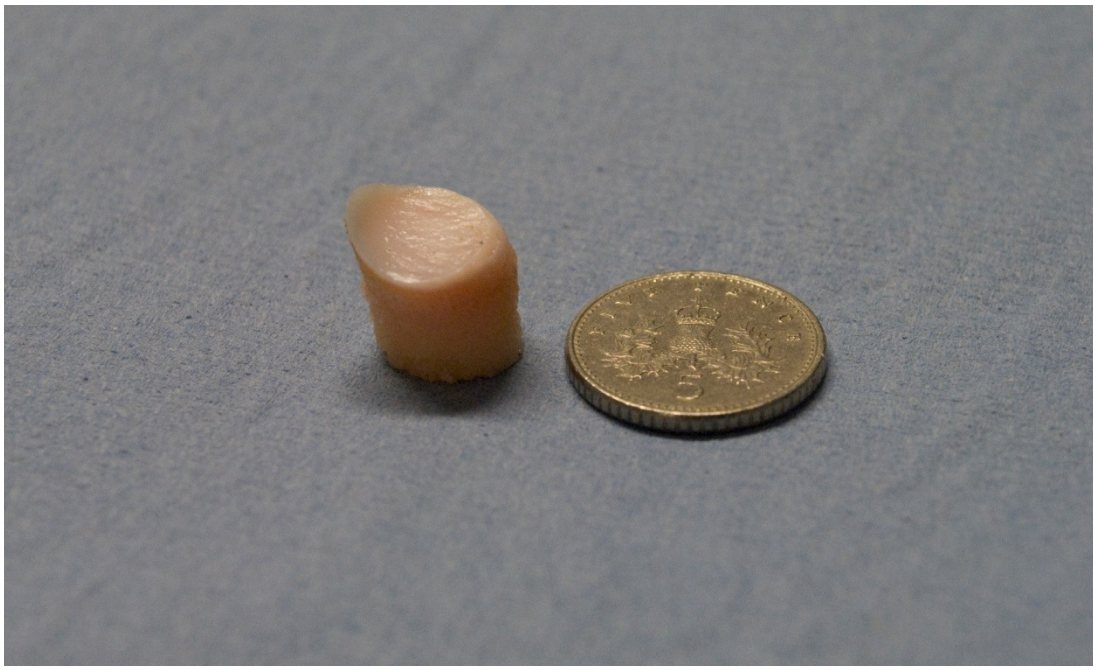

Figure 5.4: A typical 10mm cylindrical osteochondral plug.

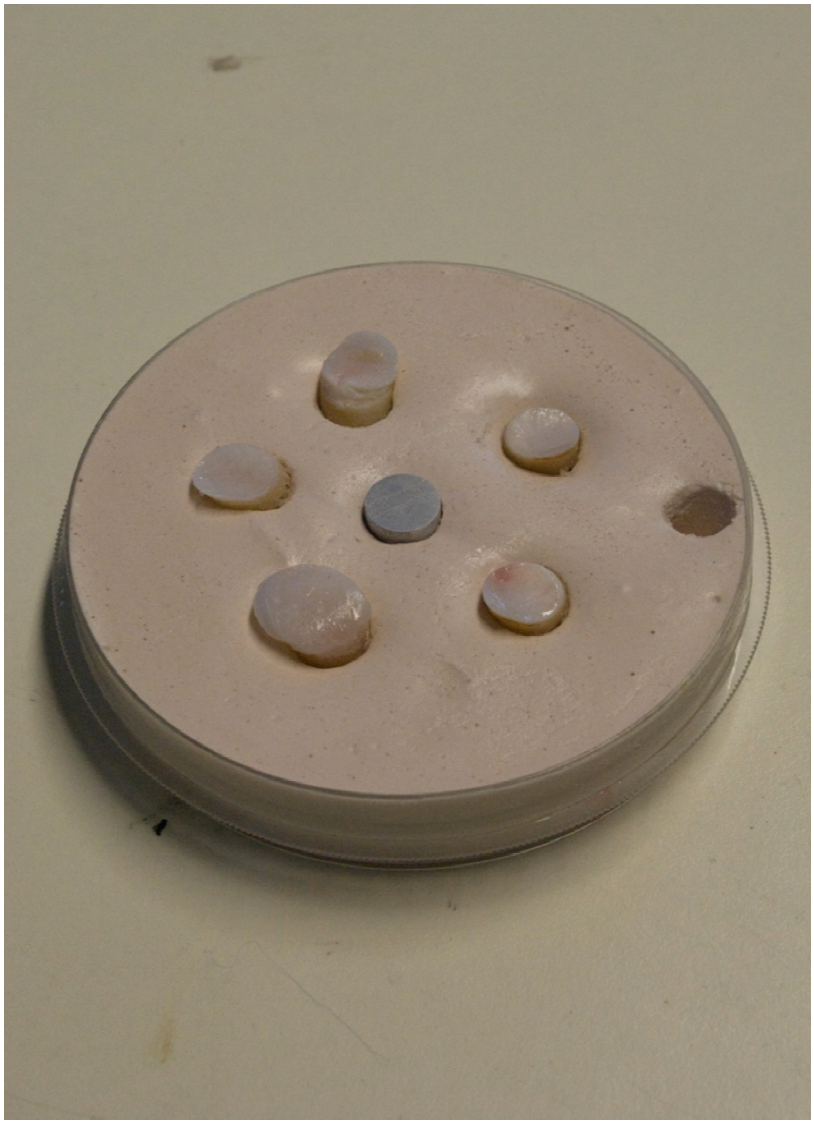

Figure 5.5: The osteochondral plugs were placed in the plaster containing petri dish.

6. Indentation Methods

6.1. Introduction

This chapter details the various experiments performed using the system detailed in chapters 3 & 4, and the tissue preparation methods presented in the previous chapter. Four experiments were performed in the following order.

1. Indentation on the metal plug;
2. Compression of the tissue samples by spherical and plane-ended indenters;
3. An investigation into the preconditioning of the cartilage; and
4. Its subsequent recovery.

6.2. Indentations on metal plugs

The main purpose of this indentation experiment to confirm that, in subsequent experiments the deformation data obtained from the sensor would originate from the osteochondral plug and not from the deformation of the plaster. A metal cylindrical plug (diameter - 10mm and height - 1cm) was placed in a petri dish containing plaster and in between some cartilage plugs (Figure 6.1). The metal plug was indented with a plane head indenter 5 times in the same spot on its surface using the methodology in section 4.3.2. If the LVDT displacement exactly equalled the actuator displacement, then it is known that the plaster and surrounding environment does not deform under the indentation load.

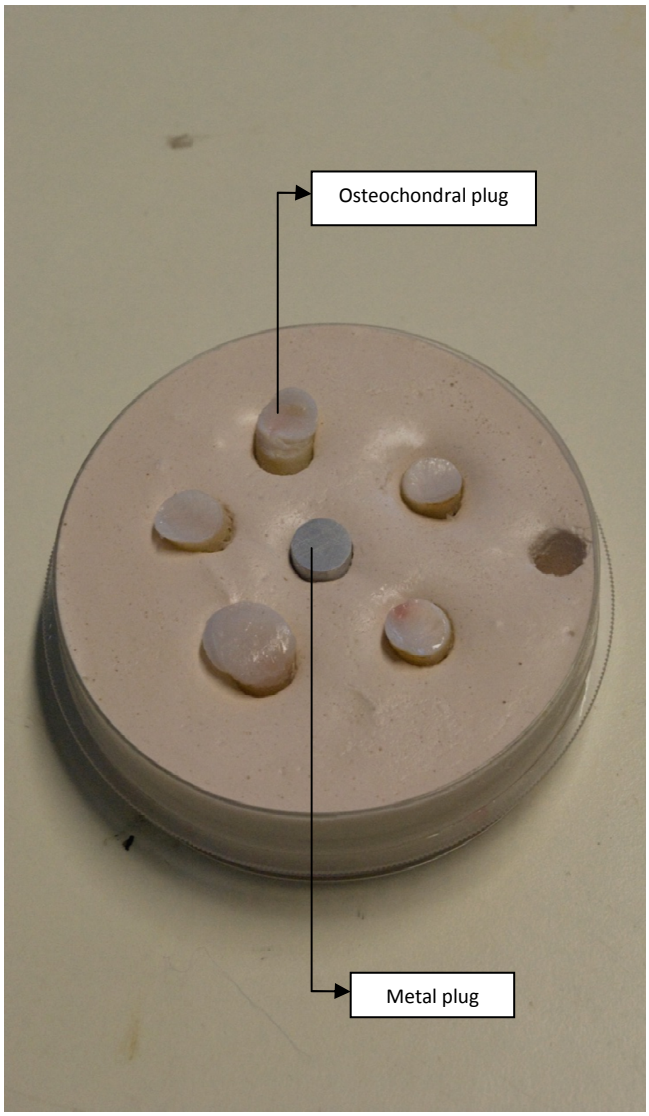

Figure 6.1: The metal plug is placed in between osteochondral plugs.

6.3. Spherical vs. Flat-headed indenter

In this section, the experimental methodology which assessed the differences between a spherical indenter and a flat ended indenter is presented.

The schematic diagram of the indentation method is shown in (Figure 2.9). The spring loaded LVDT (Linear Variable Differential Transformer) displacement sensor was connected to the linear ultra precision actuator detailed in section 3.3.2. Both spherical and plane ended rigid indenter heads were attached by a screw to the end of the LVDT. The actuator displacement speed was set to 5mm/second and the LVDT spring stiffness was 0.131 N/mm determined previously in section 3.3.2. The maximum force applied on the cartilage surface by the indenter head was 0.655 N when the actuator moves 5mm (0.131 N/mm x 5). The actuator displacement was maintained for 30 seconds and the corresponding cartilage deformation monitored by the LVDT and the applied force calculated by computer. The above testing conditions and parameters are common for both spherical and cylindrical plane ended indenters.

The spherical indenter diameter was 4.8 mm and the cylindrical plane ended indenter diameter was 5.1 mm. In total 16 osteochondral plugs were used to evaluate the cartilage deformation behaviour for both indenters; 8 specimens were used and indented 3 times in the spherical head indentation test and 8 specimens were used and indented 3 times each for the plane ended indentation test. Therefore 24 indentations were performed for each indenter type. The osteochondral plugs were placed in plaster contained in a petri dish (Figure 6.2). To best achieve a flat surface, the cartilage samples are placed in plaster and manually adjusted so that the surface was normal to the indenter. After the plaster set, the petri dish was placed under the LVDT.

Figure 6.2: The osteochondral plugs are placed in plaster contained petri dish for measuring the creep properties of the cartilage.

6.4. Preconditioning of cartilage

This section describes the experimental methodology with respect to the preconditioning of the cartilage specimens.

Osteochondral plugs (10 mm diameter) were placed in a petri dish containing plaster (Figure 6.2). The cartilage preconditioning properties were evaluated in a similar manner to section 6.3. The cylindrical plane ended indenter (5.1 mm diameter) was attached to end of the LVDT. The osteochondral plugs in the petri dish were placed under the indenter. All the measurements were recorded at the same displacement and ramp speed which are 5mm and 5mm/second respectively. The varying load produced by the LVDT spring stiffness was applied on the cartilage surface for 30 seconds. The surface displacement of cartilage was monitored by the

LVDT. Each plug was tested 10 times in exactly the same place on the cartilage surface with a time interval of 20 seconds between each test.

6.5. Recovery test of cartilage

To test how long it takes the cartilage to recover to its pre preconditioned state, the experiment in section 6.4 was repeated with the difference being that only 5 cycles of preconditioning were deemed necessary. A further 6th indentation was also done in the same place on the cartilage surface but after either 1, 5, 10, 20 or 30 minutes interval. This 6^{th} result was compared to the initial displacement. If the properties determined from the 6^{th} indentation were the same as those of the first indentation, one could say that the sample had fully recovered. The figures 7.7 to 7.11 represents the typical data obtained from 5 different time interval indentation tests performed on osteochondral plugs. For each test 5 osteochondral plugs was used and each graph obtained from average of 5 different specimens.

7. Results

7.1. Metal Plug

Indentations on the metal plug were performed to ensure that the subsequent deformations on the cartilage were that of the cartilage surface and not that of the plaster or MTS system. It is clear from Figure 7.1 that the surface of the metal plug did not relax with time, whilst the surface of the cartilage did.

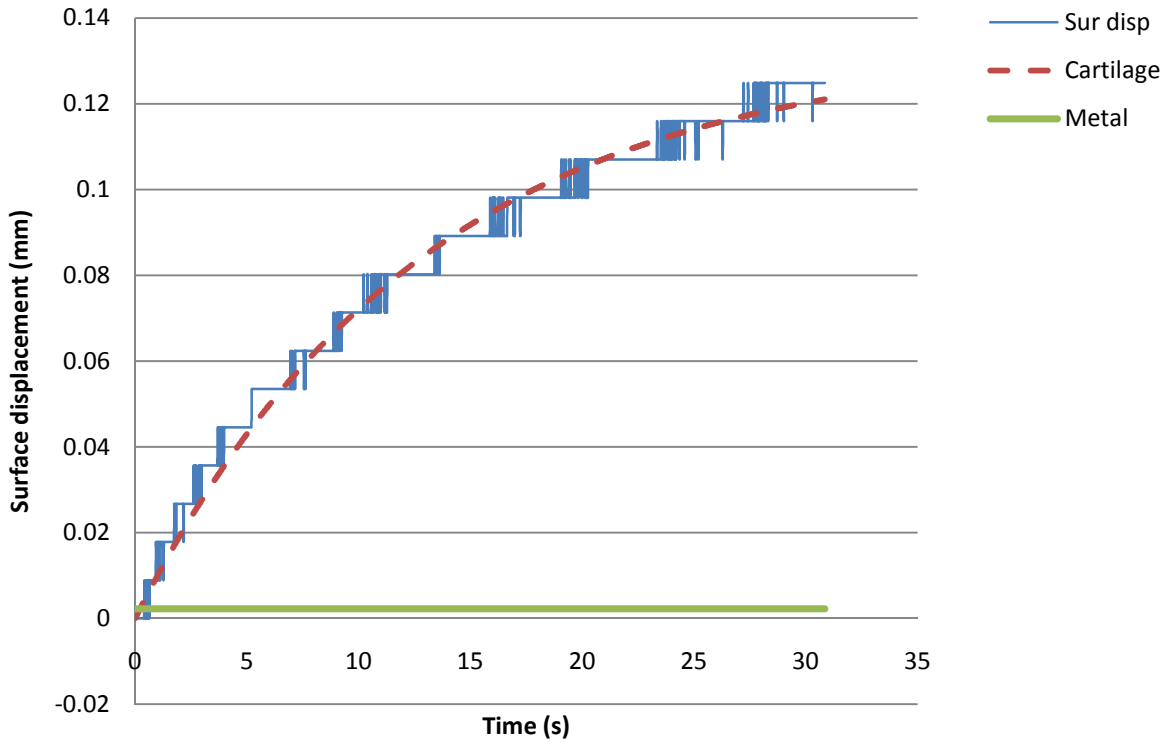

Figure 7.1: Deformation difference between metal plug and cartilage.

7.2. Spherical vs. Flat head indenter

In total, 8 osteochondral plugs were tested with the spherically headed indenter and a further 8 plugs were tested with the cylindrical plane-ended indenter. Each plug was tested three times. Data presented are therefore an average of 24 indentations. The T-test data analysis method was used to test whether the means of the two sets of indentation parameters are statistically different.

7.2.1. Spherical and flat head indenter force relaxation

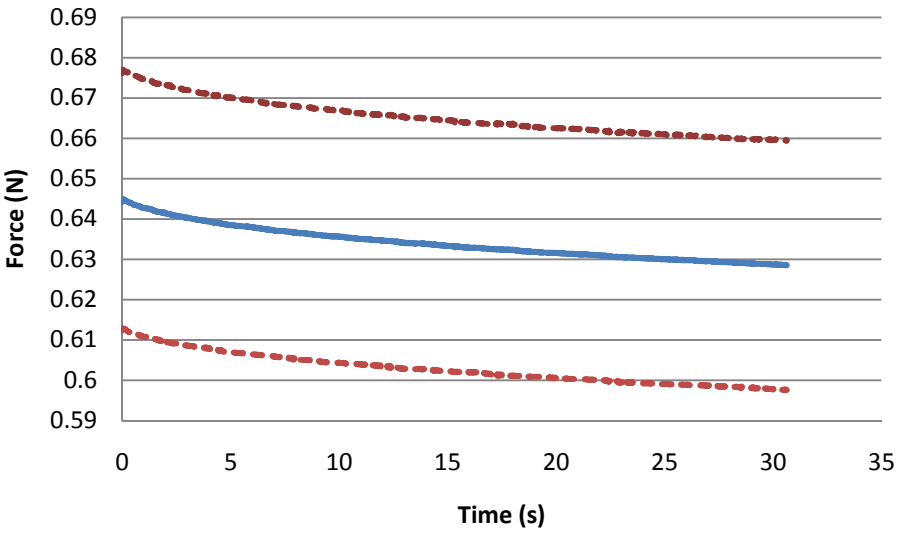

Figure 7.2: Force applied on cartilage applied through spherical indenter and the dotted lines representing ±1 standard deviation (N=24).

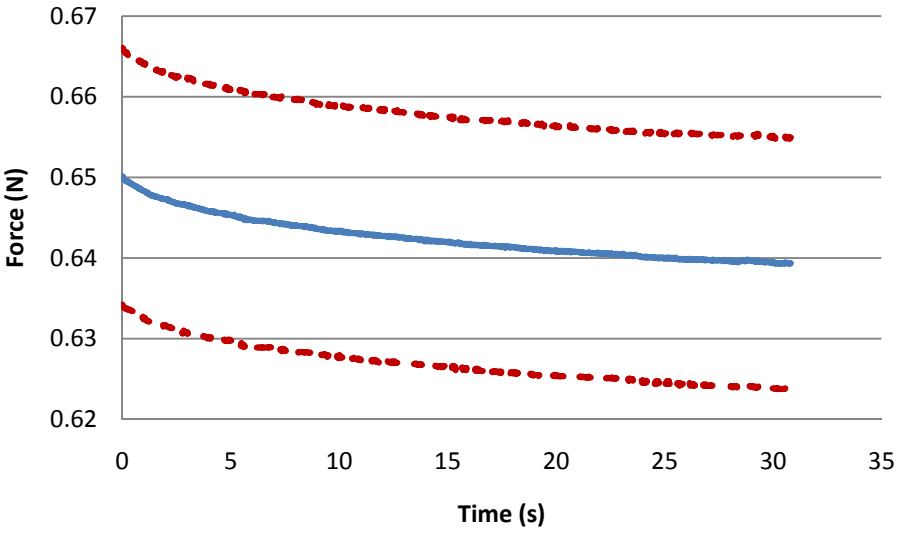

Figure 7.3: The force applied by the plane-ended indenter on cartilage surface and dotted lines representing ±1 standard deviation (N=24).

The force applied by the spherical head indenter and flat head indenter are depicted on Figure 7.2 and Figure 7.3 respectively. The spherical head indenter transferred less force on the cartilage surface during indentation test which is 0.644 N (Figure 7.2) compared to the flat-headed indenter (0.650 N, Figure 7.3)**.** The deformations proceeded until the force reached 0.628 N and 0.639 N implying that the force decreased by 0.16 N and 0.11 N respectively due to cartilage creep action.

7.2.2. Comparison of both plane-ended and spherical head indenter

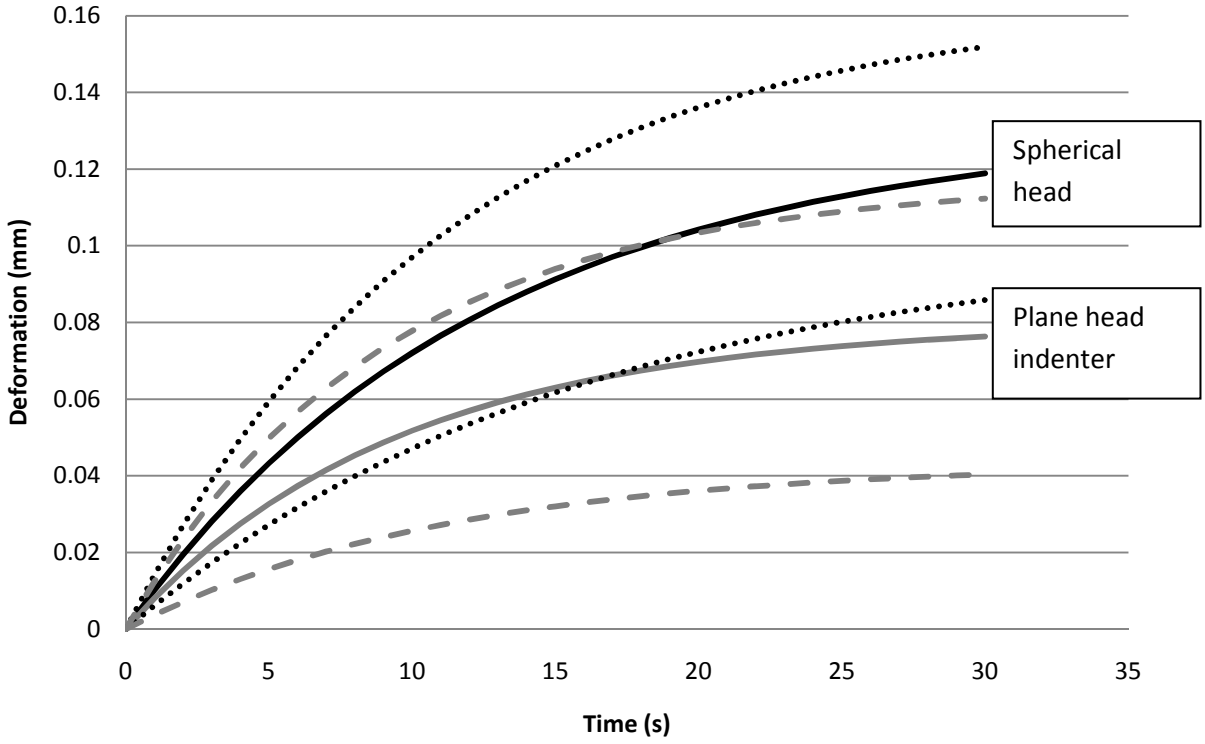

Figure 7.4: Deformation difference between spherical head indenter (solid black curve) and plane head indenter (solid grey curve) with standard deviation.

As can be seen on Figure 7.4, the spherical head indenter deforms the cartilage more quickly and produces a deeper deformation than the plane headed indenter. The displacement at the

contact region and the time constant describing the rate of displacement were significantly affected by the indenter head (Table 1, both $p < 0.05$).

Test	Spherical head indenter		Plane ended indenter	
	A_S	B_S	A_P	B_P
Mean	0.133	0.0770	0.0805	0.107
St Dev	0.0302	0.0168	0.0370	0.0290
p-Value	A_S vs. A_P 0.001		B_S vs. B_P 0.001	

Table 7.1: Experimental parameters determined from equation 1.

Table 7.1 shows that the spherical head and flat head indentation tests resulted in different equation parameters when indenting on the articular cartilage surface.

7.3. Preconditioning of cartilage

The plane-ended indenter was used for evaluating the preconditioning properties of articular cartilage. The maximum load transferred on cartilage surface was 0.655 N during the indentation time. Figure 7.5 depicts the deformation of cartilage for each cycle. Indentation depth decreased with each cycle of loading until approximately the 5^{th} cycle. After 5 cycles, the cartilage can be assumed to have preconditioned. Figure 7.6 demonstrates that the time constant, B, does not undergo any preconditioning.

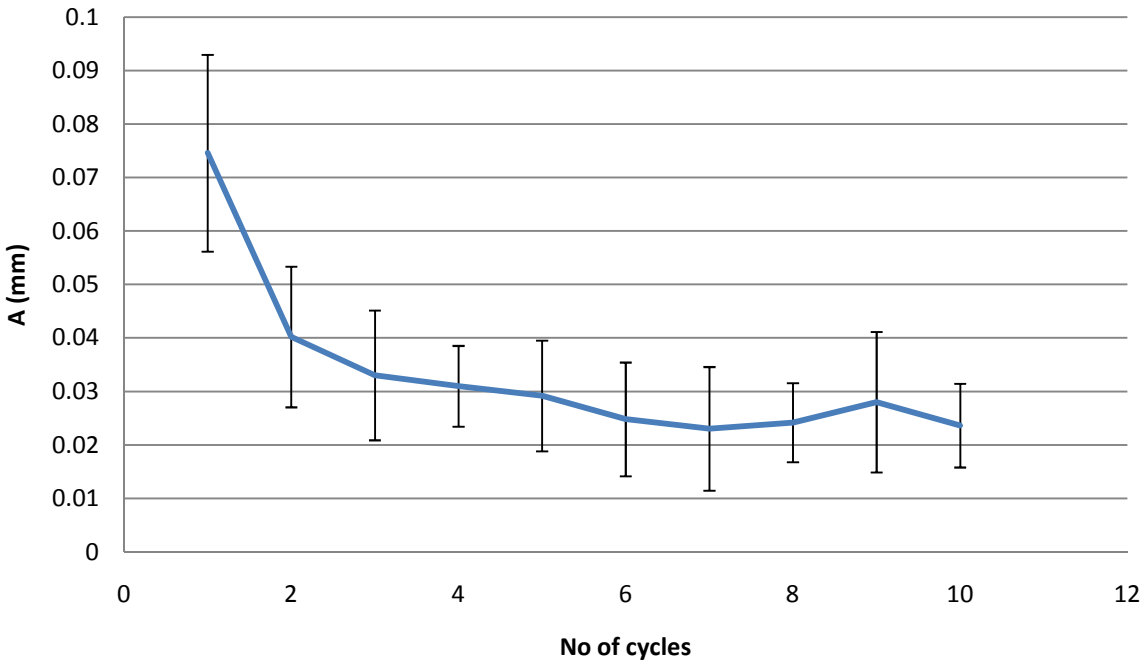

Figure 7.5: Means and standard deviations for 10 independent sets of results for A_P which explains surface deformation (plane-ended indenter).

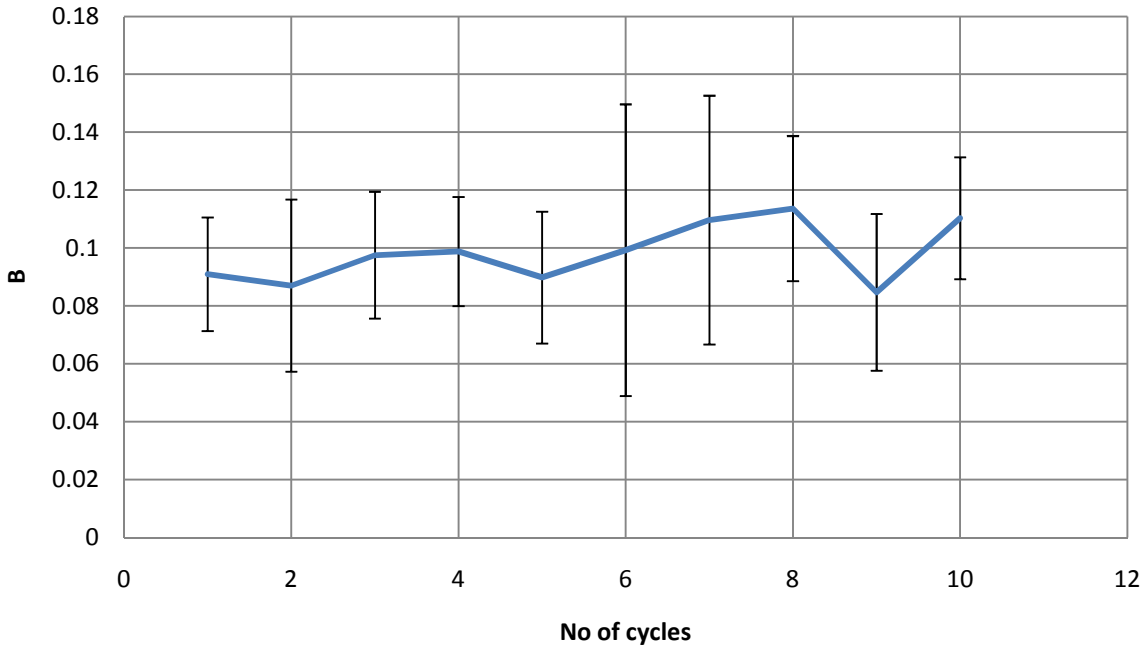

Figure 7.6: Means and standard deviations for 10 independent sets of results for parameter B_P.

7.4. Recovery of cartilage

Figures 7.5 and 7.6 indicate that the cartilage surface is fully preconditioned after approximately 5 indentations. It was desirable to know whether the pre- preconditioned state, i.e. the original state, was recoverable, and how long it may take for this to happen. The results presented in this section represent the average of 5 deformation curves at each time period. Figure 7.7 compares the 1st and 6th indentation after an interval of 1 minute between the 5th and 6th indentations. The displacement of the first indentation is 69µm, whilst 1 minute after the 5th indentation, the 6th indentation had a surface displacement of 26µm. Clearly it can be concluded that one minute is not long enough for the sample to recover to its original position.

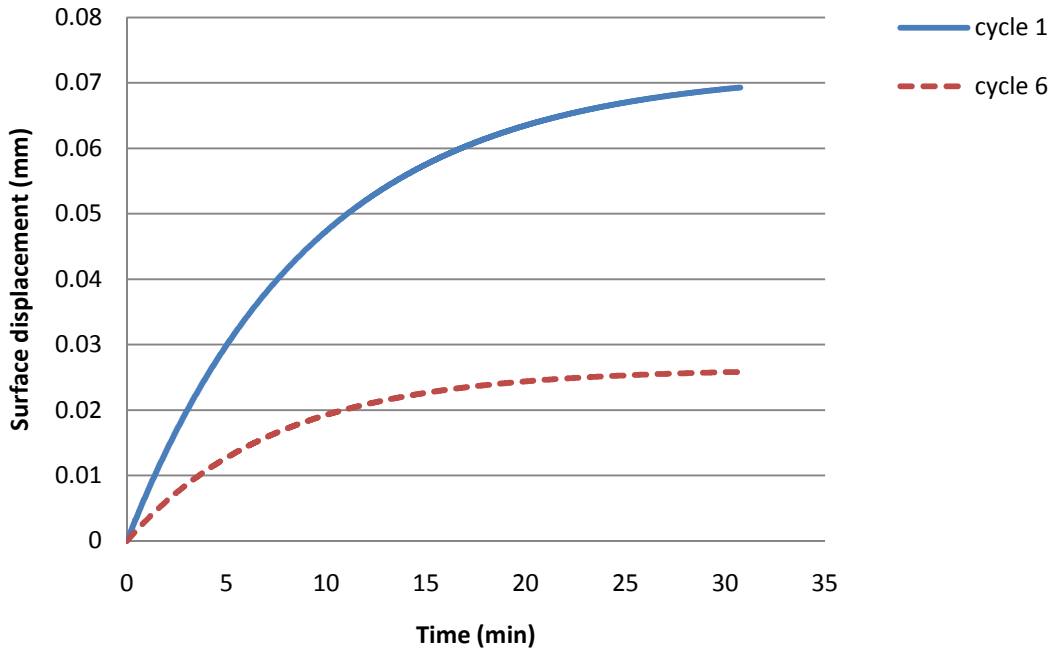

Figure 7.7: Comparison of the 1st and 6th indentations after a 1 minute period between the 5th and 6th indentations. The fitted surface displacement is plotted, with time = 0 implying initiation of contact (N = 5).

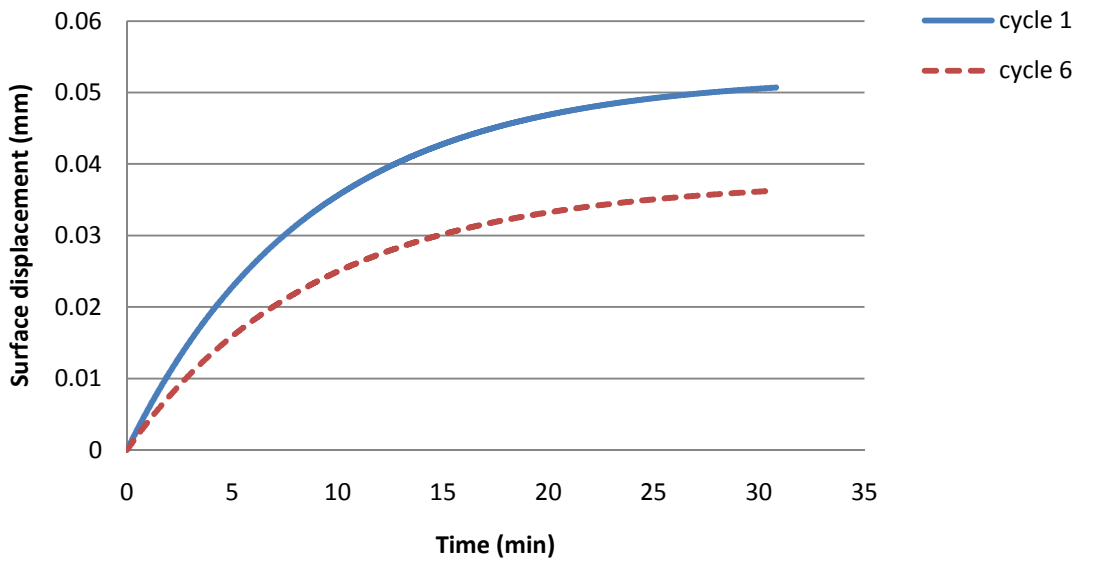

Figure 7.8: Comparison of the 1st and 6th indentations after a 5 minute period between the 5th and 6th indentations. The fitted surface displacement is plotted, with time = 0 implying initiation of contact (N = 5).

In Fig 7.8, the 6th indentation was performed after 5 minutes after the 5th indentation and compared to the 1st indentation test. The first indentation test deformation depth was 52µm (Figure 7.8) whilst the sixth indentation result was 37µm implying 5 minutes is not enough to recover to the original condition.

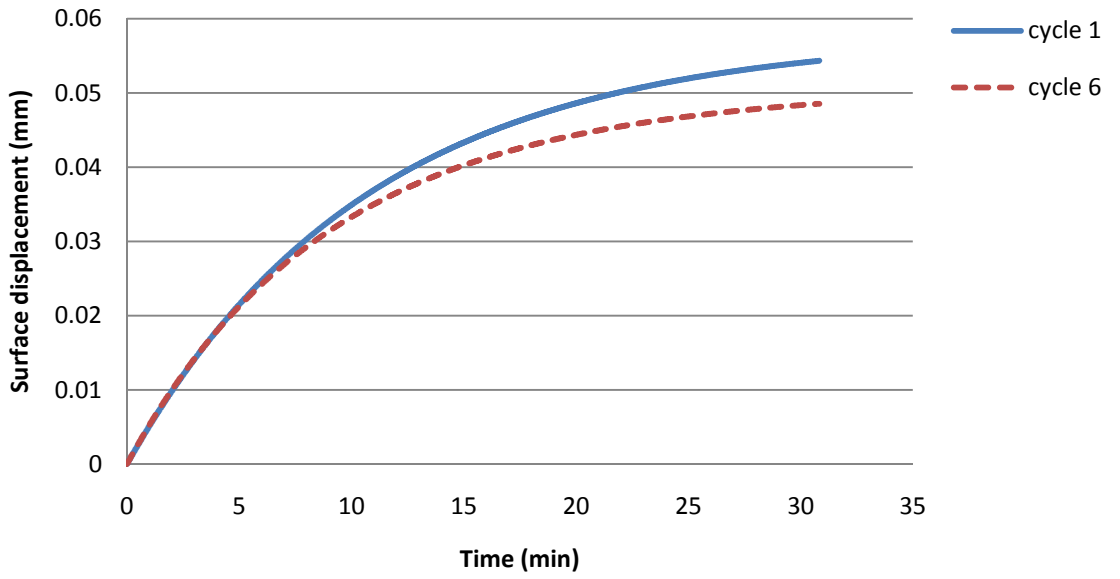

Figure 7.9: Comparison of the 1st and 6th indentations after a 10 minute period between the 5th and 6th indentations. The fitted surface displacement is plotted, with time = 0 implying initiation of contact (N = 5).

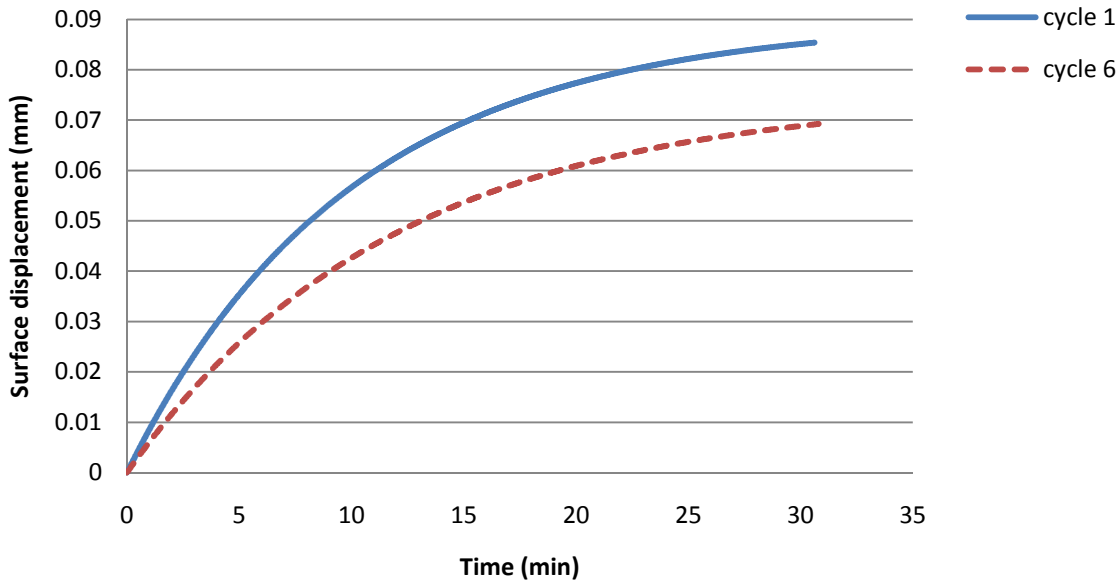

Figure 7.10: Comparison of the 1st and 6th indentations after a 20 minute period between the 5th and 6th indentations. The fitted surface displacement is plotted, with time = 0 implying initiation of contact (N = 5).

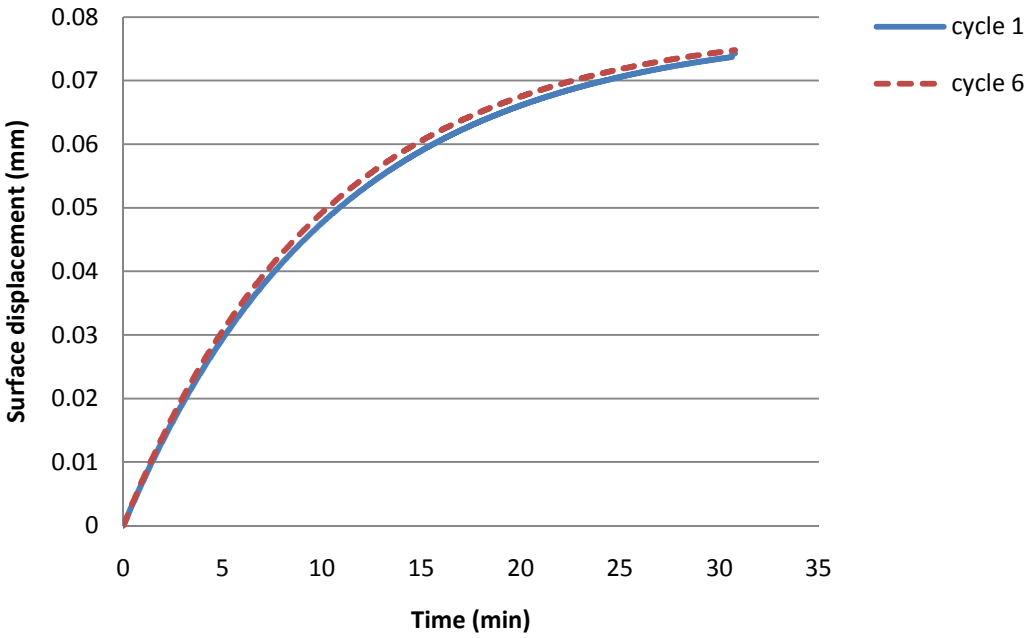

Figure 7.11: Comparison of the 1st and 6th indentations after a 30 minute period between the 5th and 6th indentations. The fitted surface displacement is plotted, with time = 0 implying initiation of contact (N = 5).

Figures 7.9, 7.10 and 7.10 present the differences between the 6th and 1st indentations after gaps of 10, 20 and 30 minutes from the 5th indentation respectively. These graphs indicate that the recovery is slow, and finally, after 30 minutes, the recovery may be complete. The preceding graphs can be summarised, as in Figure 7.12.

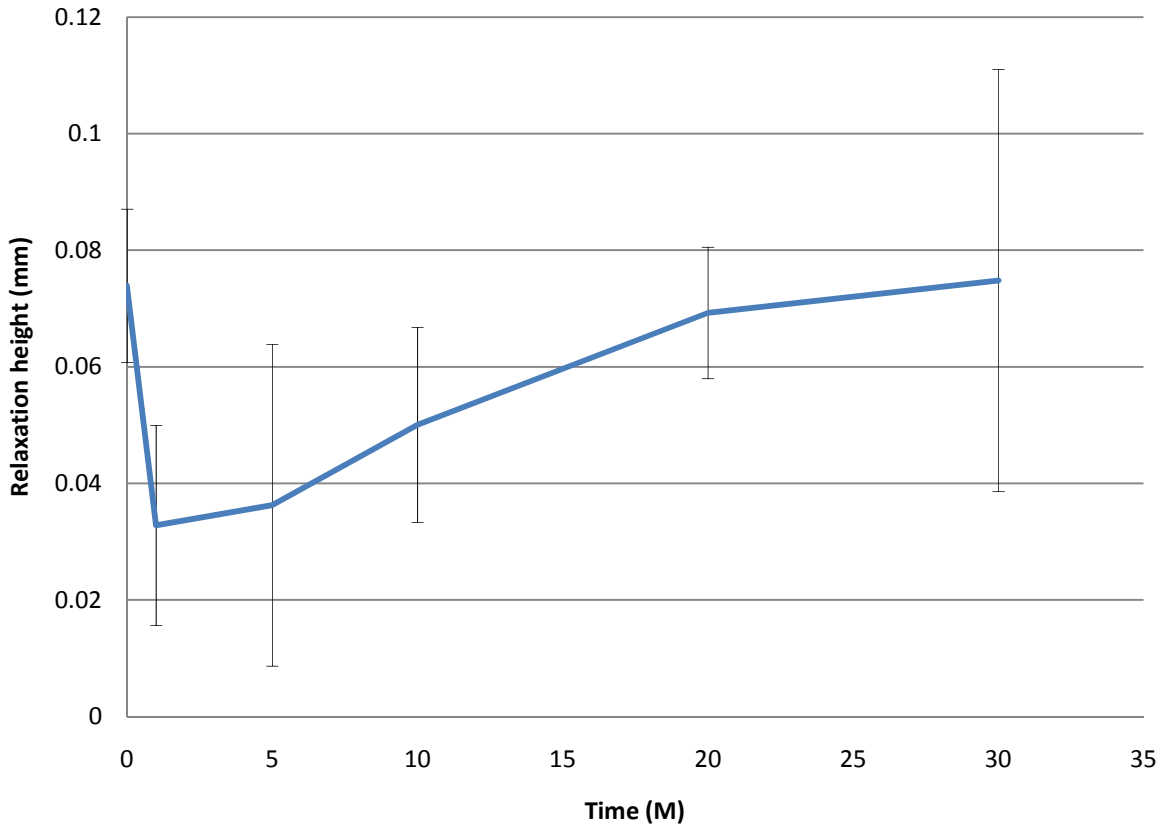

Figure 7.12: Cartilage relaxation with reference of time from 1 minute to 30 minutes. Error bars depict one standard deviation.

Figure 7.12 shows the average recovery of cartilage after preconditioning. Recovery increases with time after preconditioning and after 30 minutes the mean indentation depth is nearly the same as that of the first indentation in the preconditioning phase.

8. Discussion, conclusion and future work

8.1. Introduction

To assess and discuss the aims and objectives (section 2.6), this chapter will initially discuss the general deformation mechanism beneath an indenter in our experiments before discussing each experiment individually. The chapter ends with a discussion on the issues of the designed system; suggested further research; and a discussion pertaining to the implementation of such a system into a device for use in an operating theatre.

Before the discussion proceeds, it can be stated that the experiment conducted on the metal sample (Figure 7.1) confirmed that, as the indenter tip is forced into the surface of the material being indented, any measured deformation is that of the surface of the material, and not of the underlying plaster and rig. Consequently, we can assume that the measured deformations on the surface of the articular cartilage specimens are that of the cartilage surface and not of any other origin.

8.2. General deformation mechanism

The use of an LVDT to both provide the application of a force, as well as a measure of a displacement is an unusual, if not novel application of the spring loaded LVDT. The low spring stiffness of the LVDT ensures a low load ($\leq$0.655N) is imparted to the cartilage surface, thereby protecting the surface of the cartilage at all times.

In all the experiments presented here, the actuator drives the shaft of the LVDT at 5mm per second. This fast ramp was intended to mimic a step input. If the cartilage were rigid, then this would result in a 5mm displacement of the LVDT with the force being ramped from 0N to 0.655N in the same time period, as seen in the experiment on the metal sample. However, the "step input" was not achieved since the cartilage started to deform in the loading phase, and so the theoretical maximum force of 0.655N was rarely reached. This tissue-dependent loading regimen will make it difficult to fit any analytical solutions to biphasic models in the future. One possible solution to this issue would be to increase the actuator speed or to adjust the actuator speed during the ramp to maintain a constant loading rate. The device was designed to

utilise as low a load as possible to reduce any chance of cartilage damage. The loads are not meant to mimic loads cartilage experiences physiologically, but rather the loads a surgeon is willing to place on the cartilage intra-operatively.

Articular cartilage is somewhat more complex that the linear theory supposes and many researchers have included collagen fibre orientation and osmotic pressure in their models. The mechanical point of view the collagen and proteoglycan are main structural components of cartilage and play an important role in the health and function of the diarthroidal joint. Collagen accounts for approximately half the dry weight of articular cartilage, with the amount decreasing with depth from the articular surface (Maroudas et al., 1969; Muir et al., 1970). In contrast the proteoglycan content varies approximately inversely with the collagen content and there is a topographical variation in the overall composition of articular cartilage that appears to be characteristic of the individual (Maroudas et al., 1969; Muir et al., 1970).
According to the linear biphasic theory (Mow et al., 1980), any applied stress is balanced by a stress in the solid matrix (due to deformation), and a stress in the fluid phase. The stress in the fluid phase is equal to the negative of the pore pressure multiplied by the tissue's porosity. On immediate application of a stress via an indenter, the solid matrix does not have an instantaneous deformation since fluid has not had any time to move within the tissue, and therefore all the stress is balanced by the fluid phase (i.e. the pore pressure). Fluid then begins to flow from regions of high pore pressure to regions of low pore pressure, and as it does, the solid skeleton deforms and takes some of the load. In the case of an indentation, there is a region of high pore pressure directly beneath the indenter which dissipates radially with time. Fluid continues to flow in the tissue until there are no more fluid pressure gradients. Thus, at equilibrium the stress is being taken by the solid phase.

The solid phase incorporated of cells, fibres and a non-collagenous matrix. The fibre direction may play an important role in resisting indentations. In the centre of the tibial plateau the collagen fibrils start perpendicular to the subchondral bone (Figure 2.7 and 2.8). Just below the articular surface they bend over to merge with the articular surface. Halfway from the centre to the periphery, the collagen fibrils start bending over earlier, resulting in a thicker superficial and transitional zone. Near the periphery fibrils start in the deep zone perpendicular to the articular surface and slowly bend over to an angle of -45 and +45 degrees with the articular

surface (Wilson et al., 2006). Further work is required to assess whether there is a depth dependency to indentation testing, implying a relationship with fibre direction.

In degenerated cartilage the proportion of aggregated proteoglycans is less compared with healthy cartilage (Brandt et al., 1976; Inerot et al., 1978). Loss of proteoglycans would allow the remaining proteoglycan to become relatively more hydrated than normal. This would be expected to reduce the swelling pressure that the proteoglycan component could use (Vignon et al. 1984).

Tissue deformations in these experiments are only <100 microns, which is less than 5% of the tissue thickness. This suggests that the deformation maybe within the superficial zone where the cartilage fibres are oriented parallel to the tissue's surface. This may mean that this technique can only identify surface imperfections as opposed to deeper lesions. It must be stated, however, that early identification of surface properties is important, since degeneration and/or damage starts at the surface (Veje et al., 2003). Since the indent deformation was less than 5% of the tissue height, it is likely that the corresponding radial stresses and deformations were small. Future modelling and/or experiments are needed to confirm this assumption.

At early times in the indentation, the response of the tissue to the applied load is governed by both the permeability and the stiffness of the matrix. At stress equilibrium, tissue permeability does not affect the tissue's behaviour since no fluid is flowing. Consequently, it is only at longer times that the stiffness of the solid matrix can truly be determined. Once the stiffness of the matrix has been determined, the permeability of the matrix can be determined from the preceding time-dependent data. Frequent saline spraying was used to maintain the hydration of the cartilage as physiologic levels. One fact that was not physiologic was the temperature at which the tests were conducted. It is not known how this would affect. The results and further tests at 37ºC are thus required.

In these experiments, whilst we have not directly determined permeability and stiffness, the two constants A and B can be related to them. The constant A is the asymptotic deformation value which the surface approaches. In confined and unconfined compression, this could be directly related to the aggregate modulus (H_A) and Young's modulus (E) respectively through a simple stress-strain relationship. In indentation testing, the stress environment is more complicated since the load is balanced by tension in the collagen fibres on the surface of cartilage and compression of the matrix below the indenter. Nonetheless, the constant A could be considered a measure of stiffness where an increased stiffness would mean a reduced value of A. The constant B controls how quickly the deformation A is attained. Therefore, one can consider that an increased B would mean an increased permeability. Therefore in characterising the mechanical behaviour of cartilage, it may not be necessary to fully fit a complicated biphasic (or triphasic for that matter) equation to the data, since the simple coefficients A and B allude to and are related to stiffness and permeability respectively. If this is the case, then it may not be necessary to make the changes to the loading rate as suggested above. Research is required to determine whether these two simple coefficients vary with cartilage degeneration in a significant, understandable and repeatable manner.

8.3. Spherical versus flat ended indentation

A difference has been found between indenting with the two indenter heads. Using the spherical head indenter, the deformation is deeper (i.e. A is greater) and faster (B is greater) than using the flat-ended indenter. Upon initial application of the spherical indenter, the contact region is very small, which means that there is a higher stress on the surface compared to the flat-ended indenter.

The size of the flat-ended indenter used in our experiments was much larger than those used in other studies (2.5 mm in diameter – Li and Herzog, 2006; (0.4 mm – Bae et al., 2007; 1.5 mm - Mow et al., 1989; Suh and Spilker, 1994; 0.8 mm - Korhonen et al., 2002). According to the Li and Herzog, 2006 this increased size would increase the sensitivity of the system to evaluate

collagen degeneration in osteoarthritis. Since we did not have any other size indenter nor tested on degenerated tissue, further work may be appropriate to clarify these issues.

The cylindrical flat-ended indenter produces high axial strain around the radial edge of the indenter tip during the indentation on the cartilage implying that cell death would begin around the contact region like a ring shaped area on the cartilage surface (Bae et al., 2005). During spherical head indentation, the chondrocyte death rate is much higher than flat-ended indenter due to the deep compression and larger strain closer to centre of the indenter (Bae et al., 2007). Despite the cell death, the spherical head indenter does not make any damage on the cartilage surface due to a lack of any sharp edge. But the flat ended indenter may damage the cartilage surface around the radial edge of the indenter. In order to avoid tissue damage, it has been suggested that sharp-edged indenters should not be used (Li and Herzog, 2006).
The size of indenter is an important parameter for an arthroscopic device. If the indenter size is small ($d \leq 5$ mm) then it could be used more precisely during surgery. The spherical head indenter deformation is deeper and quicker than flat-ended indenter and seems to be safer for cartilage surface; however the flat-ended indenter produces less strain on the cartilage surface due to the larger contact region. Chondrocyte viability is of utmost significance during in vivo testing and consequently it is recommended that the largest possible flat-ended indenter with smoothed off edges should be utilised in vivo.

8.4. Preconditioning & recovery

Preconditioning has been shown to affect A, but B seems independent. This may mean that stiffness is affected by preconditioning, but permeability is not, suggesting that permeability is a constant and is not dependent on such small deformations. It is possible that structural reorganisation is occurring internally during preconditioning creating reproducibility. If the deformation is at the surface of the tissue, then the deformation would be perpendicular to the fibre direction, compressing the fibres together. If the fluid is being expressed radically beneath the indenter, compression of the fibres parallel to the surface may not have a significant effect on the radial permeability, and thus the parameter B does not show any preconditioning affect.

Cartilage is often in contact with another cartilage layer, and so in vivo the surface could be considered to be in a preconditioned condition. Therefore to test the cartilage as it would be in vivo, it may be important to precondition the sample. However, to the author's knowledge, no one has reported the effect of preconditioning on the indentation mechanics of cartilage. Our results suggest that in order to attain a reproducible value for cartilage stiffness (i.e. parameter A) multiple indentations in succession are required for this loading scheme. It was shown in the preconditioning experiment that approximately 5 indentations were required to achieve a reproducible value for A. It is hypothesised that some internal structural reorganisation may occur in the preconditioning that affects the stiffness but not the permeability. It is also important therefore to see whether the tissue returns to its original condition, after the preconditioning. The results of the recovery experiment show that the tissue recovers its original in vitro condition after around 20 to 30 minutes. However, it must be noted that these experimental conditions may not be representative of the in vivo condition as discussed above.

Many studies have reported the mechanical properties of bovine articular cartilage (Ateshian., 1997, Vunjak-Novakovic et al., 1999, Demarteau et al., 2006) and human articular cartilage (Armstrong et al., 1982, Basser et al., 1998, Demarteau et al., 2006). Moreover human hip cartilage is one of the stiffest materials among species and joints on the lower limb (Shepherd et al., 1999). However there are important differences between bovine and human cartilage. Human cartilage stiffness tends to decrease after ~50 years (Kempson., 1982) whereas bovine cartilage compressive stiffness increases with age to be maximum at adult age (Williamson et al., 2001). Hence, it may be concluded that the mechanical properties of human cartilage deteriorate with age. There are significant differences too in terms of Young's modulus (E), confined compression modulus (H_A) and permeability (k) based on its solid matrix composition (Demarteau et al., 2006). Nevertheless, the acute load – deformation mechanical response of mature human femoral cartilage and adult bovine humeral cartilage were similar against load (Demarteau et al., 2006).

8.5. Issues, further work and application

A cheap bench top indentation device has been manufactured that enables the time-dependent and static properties of cartilage and other soft tissues to be determined.

Advantages: The system utilises low load indenter which means the theoretical maximum force of 0.655N was rarely transferred on the cartilage surface through the indenter tip. Our system is able to determine two parameters (A and B) which may be related to stiffness and permeability. The system is easy to operate and user friendly, and, most importantly, it takes less than a minute to assess the cartilage quality.

Issues: Since this is a low load system, providing small surface displacements (~20 microns), the current data acquisition system does not have the requisite bit resolution; the system also uses an awkward loading profile – the load applied is dependent on the tissue response. Some feedback system may be appropriate to ensure that every tissue receives the same ramp loading condition. This would facilitate a more comprehensive mathematical analysis of the resulting data.

Further work: Investigate whether analytical or numerical mathematical solutions may be applied to the resulting data to convert the parameters A and B into stiffness and permeability values respectively. Investigate whether A and B vary with degeneration which is very important analysis to differentiate between healthy cartilage and degenerate (osteoarthritis) cartilage.

The design of rig was introduced to mimic a full size material testing machine. It is not intended to represent any machinery that would be used intraoperatively. During surgery, we currently envisage that a robotic arm replaces the rig with the linear actuator and LVDT place at the end of the arm. The loads induced are so small that hopefully there is a realistic chance that motion of the robotic arm with repeat to the knee is less than the surface deformation of the cartilage. Only testing will answer this important question.

Application: The actuator and displacement sensor unit needs to be implemented into a hand-held device or robotic arm for arthroscopic use. Need to know precisely where the actuator is at all times to high accuracy. This may be the downfall for this system. On a hand held device this

would be highly problematic, but a robotic arm may be more rigid. An increase in the force applied would increase the depth of the indentation, which would lessen the accuracy requirement of the device; however this has the counterproductive issue of potential tissue damage.

9. References

Adams MA (2006) The mechanical environment of chondrocytes in articular cartilage, Biorheology, 43, 537-545.

Al-ja'afreh T, Zweiri Y, Seneviratne L and Althoefer K (2008) A new soft-tissue indentation model for estimating circular indenter 'force-displacement' characteristics, Journal of Engineering in Medicine, 222, 805-815.

Appelman TP , Mizrahi J , Elisseeff JH , Seliktar D (2009) The differential effect of scaffold composition and architecture on chondrocyte response to mechanical stimulation, Journal of Biomaterials, 30, 518-525.

Armstrong CG and Mow VC, Troy (1982) Variations in the Intrinsic Mechanical Properties of Human Articular Cartilage with Age, regeneration, and Water Content, The Journal of Bone and Joint Surgery, 88-94.

Armstrong CG, Lai WM and Mow VC (1984) An analysis of the unconfined compression of articular cartilage, Journal of Biomechanics, 106, 165-173.

Ateshian GA, Warden WH, Kim JJ, Grelsamer RP and Mow VC (1997) Finite Deformation Biphasic Material Properties Of Bovine Articular Cartilage From Confined Compression Experiments, Journal of Biomechanics, 30, 1157-1164.

Athanasiou KA, Rosenwasser MP, Buckwalter JA, Malinin STI and Mow VC (1991) Interspecies Comparisons of In Situ Intrinsic Mechanical Properties of Distal Femoral Cartilage, Journal of Orthopaedic Research, 9, 330-340.

Bae WC, Lewis CW, Levenston ME, Sah RL (2006) Indentation testing of human articular cartilage: Effects of probe tip geometry and indentation depth on intra-tissue strain, Journal of Biomechanics, 39, 1039-1047.

Bae WC, Schumacher BL and Sah RL (2007) Indentation probing of human articular cartilage: Effect on chondrocyte viability, Journal of Osteoarthritis and Cartilage, 15, 9-18.

Brodsky B and Ramshaw JAM (1997) Collagen Triple-Helix Structure, Matrix Biology Vol. 15/1997, 545-554.

Barbucci R (2002) Integrated Biomaterials Science, Springer, New York.

Barker MK and Seedhom BB (1997) Articular cartilage deformation under physiological cyclic loading-apparatus and measurement technique, Journal of Biomechanics, 4, 377-381.

Basser PJ, Schneiderman R, Bank RA, Wachtel E and Maroudas A (1998) Mechanical Properties of the Collagen Network in Human Articular Cartilage as Measured by Osmotic Stress Technique, Archives of Biochemistry and Biophysics, 351, 207–219.

Brandt KD, Palmoski M and Perricone E (1976) Aggregation of cartilage proteoglycans. II Evidence for the presence of a hyaluronate-binding region on proteoglycans

Buckwalter JA and Mankin HJ (1997) Articular cartilage: degeneration and osteoarthritis, repair, regeneration, and transplantation, Journal of Joint and Bone surgery, 79-A, 612-632.

Bullough and Goodfellow (1968) The Signification Of The Fine Structure Of Articular Cartilage, The Journal of Bone and Joint Surgery, 50-B, 852.

Butler DL, Goldstein SA, Guilak F (2000) Functional tissue engineering: the role of biomechanics, Journal of Biomechanical Engineering, 122, 570 - 575.

Chen AC, Nguyen TT, and Sah RL (1997) Streaming Potentials during the Confined Compression Creep Test of Normal and Proteoglycan-Depleted Cartilage, Annals of Biomedical Engineering, 25, 269-277.

Cooper C, Snow S, McAlindon TE, Kellingray S, Stuart B, Coggon D (2000) Risk factors for the incidence and progression of radiographic knee osteoarthritis, Journal of Arthritis & Rheumatism, 43, 995 –1000.

Davis MA, Ettinger WH, Neuhaus JM and Hauck WW(1988) Sex differences in osteoarthritis of the knee. The role of obesity, American Journal of Epidemiology, 127, 1019–1030.

Demarteau O, Pillet DL, Inaebnit A, Borens O and Quinn TM (2006) Biomechanical characterization and in vitro mechanical injury of elderly human femoral head cartilage: comparison to adult bovine humeral head cartilage, Journal of Osteoarthritis and Cartilage, 14, 589-596.

Duda GN, Kleemann RU, Blueche U and Weiler A (2004) A New Device to Detect Early Cartilage Degeneration, The American Journal of Sports Medicine, 32, 693-697.

Ebenstein DM and Pruitt LA (2006) Nanoindentation of biological materials, Journal of Nanotoday, 1, 26-33.

Eckstein F, Tieschky M, Faber S, Englmeier KH and Reiser M (1999) Functional analysis of articular cartilage deformation, recovery, and fluid flow following dynamic exercise in vivo, Journal of Anatomy and Embryology, 200, 419-424.

Edelsten L, Jeffrey JE, Burgin LV, Aspden RM (2008) Viscoelastic properties of articular cartilage subjected to impact loading in vitro, Journal of Biomechanics, 41(S1).

Eyre D (1990) Structure and function of the cartilage collagen: role of type IX in articular cartilage. In: Brandt. KD. (Ed.), Cartilage Changes in Osteoarthritis. Indianapolis: Ciba-Geigy,12–16.

Federico S, Herzog W, Wu JZ, Rosa GL (2004) A method to estimate the elastic properties of the extracellular matrix of articular cartilage, Journal of Biomechanics 37, 401-404.

Felson DT and Neogi T (2004) Osteoarthritis: Is It a Disease of Cartilage or of Bone?, Journal of the American College of Rheumatology, 50, 341-344.

Felson DT, Anderson J, Kazis L, Castelli W, Meenan RF (1987) The prevalence of knee osteoarthritis in the elderly (The Framingham Osteoarthritis study), Journal of Arthritis & Rheumatism, 30, 914–918.

Felson DT (1990) Osteoarthritis, Rheumatic Disease Clinics of North America, 16(3), 499–512.

Forriol F (2009) Growth factors in cartilage and meniscus repair, Journal of Injury, 40, S12-S16.

Franke OK, Maier DV, Go¨ken M, Birkholz T, Schneider H, Hennig F, Gelse K (2007) Mechanical properties of hyaline and repair cartilage studied by nanoindentation, Journal of Actabiomaterialia, 3, 873-881.

Frankel VH and Nordin M (1980) Basic biomechanics of the skeletal system, Lea & Febiger, Philadelphia.

Franz T, Mainil-Varlet P, Hasler E, Hagg R, Weiler C, Mueller W, Jakob R, Schaffner T (2000) In situ compressive stiffness and structural integrity of human articular cartilage, 46th Annual Meeting, Orthopaedic Research Society, Orlando, Florida.

Freeman MAR (1979) Adult articular cartilages – Second edition, J. B. Lippincott Company, Philadelphia, from osteoarthritis cartilage, Journal of Arthritis and Rheumatism, 19, 1308-1314.

Fulcher GR, Hukins DWL and Shepherd DET (2009) Viscoelastic properties of bovine articular cartilage attached to subchondral bone at high frequencies, BMC Musculoskeletal Disorders, 10:61, 1-7.

Fung YC (1993) Biomechanics: Mechanical properties of living tissues. 2nd ed, Springer, New York.

Guilak F (2000) The deformation behaviour and viscoelastic properties of chondrocytes in articular cartilage, Journal of Biorheology, 37, 27-44.

Hagiwara H (1992) Localization of collagen type VI in articular cartilage of young and adult mice, Journal of Cell Tissue research, 272, 155-160.

Hainsworth SV and Page TF (1994) Nanoindentation studies of chemo mechanical effects in thin-film coated systems, Journal of Surface Coating Technology, 68, 571–575.

Hangody L and Füles P (2003) Autologous Osteochondral Mosaicplasty for the Treatment of Full-Thickness Defects of Weight-Bearing Joints: Ten Years of Experimental and Clinical Experience, Journal of Bone Joint Surgery, 85, 25-32.

Hangody L, Ráthonyi GK, Duska Z, Vásárhelyi G, Füles P and Módis L (2004) Autologous Osteochondral Mosaicplasty. Surgical Technique, Journal of Bone Joint Surgery, 86, 65-72.

Hayes WC, Keer LM, Herrmann G and Mockros LF (1972) A mathematical analysis for indentation tests of articular cartilage, Journal of Biomechanics, 5, 541-551.

Heath CA and Magar SR (1995) Mini-Review: Mechanical Factors Affecting Cartilage Regeneration in Vitro, Biotechnology and Bioengineering, 50, 430-437.

Heluck AF, Lukas HP, Kohl HP (1989) Structure, function, and degeneration of bovine hyaline cartilage: assessment with MR imaging in vitro, Journal of Radiology, 170, 495-499.

Hodge WA, Fujant RS, Carlsont KL, Burgesst RG, Harris WH and Mannt RW (1986) Contact pressures in the human hip joint measured in vivo, Journal of Proceeding of the natural academy of science, 83, 2879-2883.

Hunziker EB (1999) Biologic repair of articular cartilage. Defect models in experimental animals and matrix requirements, Journal of Clinical Orthopaedics and Related Research, 367, S135-S146.

Hunziker EB (2001) Articular cartilage repair: basic science and clinical progress. A review of the current status and prospects, Osteoarthritis and Cartilage 10, 432-463.

Hutmacher DW, Ng KW, Kaps C, Sittinger M, Klaring S (2003) Elastic cartilage engineering using novel scaffold architectures in combination with a biomimetic cell carrier, Journal of Biomaterials 24, 4445-4458.

Inerot S, Heinegard D, Audell L and Olsson SE (1978) Articular-cartilage proteoglycans in aging and osteoarthritis, Journal of Biochemical, 169, 143-156.

Jadin KD, Wong BL, Li KW, Bae WC, Williamson AK, Schumacher BL, Price JH, Sah RL (2003) Depth-associated variation in chondrocyte density in bovine articular cartilage during growth and maturation, 49th Annual Meeting of the Orthopaedic Research Society, Poster 0469.

Jeffery AK, Blunn GW, Archer CW, Bentley G (1991) Three dimensional collagen architecture in bovine articular cartilage, Journal of Bone Joint Surgery, 73, 795–801.

Julkunen P, Korhonen RK , Herzog W, Jurvelin JS (2008) Uncertainties in indentation testing of articular cartilage: A fibril-reinforced poroviscoelastic study, Journal of Medical Engineering and Physics, 30, 506-515.

Julkunen P, Wilson W, Jurvelin JS, Rieppo J, Cheng-Juan Qu (2008) Stress–relaxation of human patellar articular cartilage in unconfined compression: Prediction of

mechanical response by tissue composition and structure, Journal of Biomechanics, 41, 1978–1986.

Kempson GE, Freeman MA and Swanson SA (1971) The determination of a creep modulus for articular cartilage from indentation tests of the human femoral head. Journal of Biomechanics, 4, 239-250.

Kiefer GN, Sundby K, McAllister D, Shrive NG, Frank CB, Lam T, Schachar NS (1989) The effect of cryopreservation on the biomechanical behaviour of Bovine articular cartilage, Journal of Orthopaedic, 7, 494-501.

Korhonen RK, Laasane M, T.oyr.as J, Rieppo J, Hirvonen J,Helminen HJ, Jurvelin JS (2002) Comparison of the equilibrium response of articular cartilage in unconfined compression, confined compression and indentation, Journal of Biomechanics, 35, 903-909.

Korhonen RK, Wong M, Arokoski J, Lindgren R, Helminen HJ, Hunziker EB, Jurvelin JS (2002) Importance of the superficial tissue layer for the indentation stiffness of articular cartilage, Medical Engineering and Physics, 24, 99-108.

Kuijer R, Stadt VRJ, Margret HMT,Koning DE, Jos van Kampen GP and van der Korst JK (1988) Influence of Cartilage Proteoglycans on Type II Collagen Fibrillogenesis, Journal of Connective tissue research, 17, 83-97.

Kunkel ME, Moral AI, Rilk M, Wahl FM (2007) Influence of preconditioning on the relaxation behaviour of porcine septal cartilage using different sized indenters, Journal of Biomechanics 40 (S2).

Kwan MK, Wayne JS, Woo SLY, Field FP, Hoover J, Meyers M (1989) Histological and biomechanical assessment of the articular cartilage from stored osteochondral cell allografts, Journal of Orthopaedic Research, 7, 637-644.

Lai WM, Hou JS and Mow VC (1991) A Triphasic Theory for the Swelling and Deformation Behaviours of Articular Cartilage, Journal of Biomechanics, 113, 245-259.

Laure Ng, Han-Hwa Hung, Sprunt A, Chubinskaya S, Ortiz C, Grodzinsky A (2007) Nanomechanical properties of individual chondrocytes and their developing growth factor-stimulated pericellular matrix, Journal of Biomechanics, 40, 1011-1023.

Lawrence RC, Helmick CG, Arnett FC (1998) Estimates of the prevalence of arthritis and selected musculoskeletal disorders in the United States, Journal of Arthritis & Rheumatism, 41, 778-799.

Li LP and Herzog W (2004) Strain-rate dependence of cartilage stiffness in unconfined compression: the role of fibril reinforcement versus tissue volume change in fluid pressurization, Journal of Biomechanics, 37, 375-382.

Li LP and Herzog W (2006) Arthroscopic evaluation of cartilage degeneration using indentation testing—Influence of indenter geometry, Journal of Biomechanics, 21, 420-426.

Li LP, Buschmann MD and Shirazi-Adl A (2002) The role of fibril reinforcement in the mechanical behavior of cartilage, Journal of Biorheology, 39, 89-96.

Li LP, Korhonen RK, Iivarinen J, Jurvelin JS, Herzog W (2008) Fluid pressure driven fibril reinforcement in creep and relaxation tests of articular cartilage, Journal of Medical Engineering & Physics, 30, 182-189.

Lorenz H and Richter W (2006) Osteoarthritis: Cellular and molecular changes in degenerating cartilage, Progress in Histochemistry and Cytochemistry, 40, 135-163.

Lu Xin L and Mow VC (2008) Biomechanics of Articular Cartilage and Determination of Material Properties, Journal of the American College of Sports Medicine, 193-199.

Lyyra-Laitinen T, Niinimaki M, Toyras J, Lindgren R, Kiviranta I and Jurvelin JS (1999) Optimization of the arthroscopic indentation instrument for the measurement of thin cartilage stiffness, Physics in Medicine and Biology 44, 2511-2524.

Mankin HJ and Lippiello L (1971) The glycosaminoglycans of normal and arthritic cartilage. Journal of Clinical Investigation, 50, 1712-1719.

Mansour JM, Mow VC (1976) The permeability of articular cartilage under compressive strain and at high pressures, Journal of Bone Joint Surgery, 58, 509-516.

Mansour JM (2003) Biomechanics of cartilage, in C.A. Oatis, Ed., Kinesiology: The Mechanics and Pathomechanics of Human Movement, Philadelphia: Lippincott Williams and Wilkins, chapter 5, 2003, 66-79.

Marcacci M, Kon E, Zaffagnini S and Visani A (1999) Use of autologous grafts for reconstruction of osteochondral defects of the knee, Journal of Orthopedics, 22(6), 595-600.

Marieb EN, Hoehn K (2007) Human anatomy & physiology, 7th edition, Pearson Benjamin cummings, San Francisco, CA.

Maroudas A, Bullough P, Swanson SA, Freeman MA (1968) The permeability of articular cartilage, Journal of Bone and Joint Surgery, 50, 166-177.

Maroudas A, Muir H and Wingham J (1969) The correlation of fixed negative charge with glycosaminoglycans content of human articular cartilage, Journal of Biochemistry, Biophysics and Molecular Biology, 177, 492-500.

Maroudas A, Schneiderman R (1987) "Free" and "exchangeable" or "trapped" and "non-exchangeable" water in cartilage, Journal of Orthopaedic Research, 5, 133-138.

Maroudas A (1976) Balance between swelling pressure and collagen tension in normal and degenerate cartilage, Journal of Nature, 260, 808 – 809.

Martin BR, Burr DB, Sharkey NA (1998) Skeletal tissue mechanics, Springer-Verlag, New York.

Mithoefer K, Williams RJ, Warren RF, Potter HG, Spock CR, Jones EC, Wickiewicz TL and Marx. RG (2005) The micro fracture technique for the treatment of articular cartilage lesions in the knee. A prospective cohort study. Journal of Bone Joint Surgery, 87, 1911-1920.

Mow VC and Huiskes R (2005) Basic orthopaedic biomechanics and mechanobiology, 3rd edition, Lippincott Williams & Wilkins, Philadelphia.

Mow VC, Sun DN, Guo XE, Likhitpanichkul M and Lai WM (2002) Fixed negative charges modulate mechanical behaviour and electrical signals in articular cartilage under unconfined compression-A triphasic paradigm, Springer, Newyork, 227-247.

Mow VC, Kuei SG, Lai WM and Armstrong CG (1980) Biphasic creep and stress relaxation of articular cartilage in compression: theory and experiments, Journal of Biomedical Engineering, 102, 73-83.

Muir H (1995) The chondrocyte, architect of cartilage. Biomechanics, structure, function and molecular biology of cartilage matrix macromolecules, Journal of Bioessays, 17(12), 1039-1048.

Muir H, Bullough P and Maroudas A (1970) The distribution of collagen in human articular cartilage with some of its physiological implications, Journal of Bone and Joint Surgery, 52B, 554-563.

Newman AP (1998) Articular Cartilage Repair, The American Journal of Sports Medicine, 26, 310-324.

Niederauer MQ, Cristante S, Niederauer GM, Wilkes RP, Singh SM, Messina DF, Walter MA and Boyan BD (1998) A novel instrument for quantitatively measuring the stiffness of articular cartilage, Transactions of the Orthopaedic Research Society 23, 905.

Palmer JL, Bertone AL, Mansour J, Carter BG and Malemud TCJ (1995) Biomechanical Properties of Third Carpal Articular Cartilage in Exercised and Nonexercised Horses, Journal of Orthopardrc Research, 13, 854-860.

Palmoski MJ, Brandt KD (1984) Effects of static and cyclic compressive loading on articular cartilage plugs in vitro, Journal of Arthritis Rheumatology, 27, 675-681.

Parsons JR and Black J (1977) The viscoelastic shear behaviour of normal rabbit articular cartilage, Journal of Biomechanics, 10, 21-29.

Perie D, Korda D, Iatridis JC (2005) Confined compression experiments on bovine nucleus pulposus and annulus fibrosus: sensitivity of the experiment in the determination of compressive modulus and hydraulic permeability, Journal of Biomechanics, 38, 2164-2171.

Provenzano P, Lakes R, Keenan T and Vanderby RJ (2001) Nonlinear Ligament Viscoelasticity, Journal of Biomedical Engineering, 29, 908-914.

Redman SN, Oldfield SF and Archer CW (2005) Current strategies for articular cartilage repair, Journal of European cells and material, 9, 23-32.

Risbud MV and Sittinger M (2006) Tissue engineering: advances in in vitro cartilage generation, Journal of TRENDS in Biotechnology, 20, 351-356.

Rohlmann. A and Kölbel. R, 1987, Biomechanics: basic and applied research, Springer, New York.

Sah RL, Kim YJ, Doong RY, Grodzinsky AJ, Plaas AH and Sandy JD (1989) Biosynthetic response of cartilage explants to dynamic compression. Journal of Orthopaedics, 7, 619–636.

Sakamoto M, Li G, Toshiaki Hara and Ed. Chao YS (1996) A new method for theoretical analysis of static indentation test, Journal of Biomechanics, 5, 679-685.

Schachar NS, Novak K, Muldrew K, Zernicke RF and McGann LE (1999) Articular cartilage joint surface reconstruction techniques, Journal of Orthopaedic science, 4, 457-461.

Schinagl RM, Gurskis D, Chen AC and Sah RL (1997) Depth-Dependent Confined Compression Modulus of Full-Thickness Bovine Articular Cartilage, The Journal or Bone and Joint Surgery, 15, 499-506.

Schultz W and Göbel D (1999) Articular cartilage regeneration of the knee joint after proximal tibial valgus osteotomy: a prospective study of different intraand extra-articular operative techniques, Journal of Knee Surgery, Sports Traumatology, Arthroscopy, 7, 29-36.

Smith CL and Mansour JM (2000) Indentation of an osteochondral repair: sensitivity to experimental variables and boundary conditions, Journal of Biomechanics 33, 1507-1511.

Soltz MA and Ateshian GA (2000) Interstitial Fluid Pressurization During Confined Compression Cyclical Loading of Articular Cartilage, Journal of Biomedical Engineering, 28, 150–159.

Thornton GM, Frank CB and Shrive NG (2001) Ligament creep behavior can be predicted from stress relaxation by incorporating fiber recruitment, Journal of Rheology, 45(2), 493-507.

Toyras J, Korhonen RK, Voutilainen T, Jurvelin JS, Lappalainen R (2005) Improvement of Arthroscopic Cartilage Stiffness Probe Using Amorphous Diamond Coating, Journal of Biomedical material research, 73B, 15-22.

Toyras J, Lyyra-Laitinen T, Niinimaki M, Lindgren R, Nieminen MT, Kiviranta I, Jurvelin JS (2000) Estimation of the Young's modulus of articular cartilage using an arthroscopic indentation instrument and ultrasonic measurement of tissue thickness, Journal of Biomechanics, 34, 251-256.

Trattnig S (1997) Overuse of hyaline cartilage and imaging, Journal of Radiology, 25, 188-198.

Urban JPG, Maroudas A, Bayliss MT and Dillon J (1979) Swelling pressures of proteoglycans at the concentrations found in cartilaginous tissues. Journal of Biorheology, 16, 447-464.

Veje K, Hyllested-Winge JL and Ostergaard K (2003) Topographic and zonal distribution of tenascin in human articular cartilage from femoral heads: normal versus mild and severe Osteoarthritis, Journal of OsteoArthritis and Cartilage, 11, 217–227.

Vignon E, Hartman JD, Vignon E, Moyen B, Arlot M and Ville G (1984) Cartilage destruction in experimentally induced osteoarthritis. Journal of Rheumatology, 11, 202-207.

Vunjak-Novakovic G, Martin I, Obradovic B, Treppo S, Grodzinsky AJ, Langer R and Freed LE (1999), Bioreactor Cultivation Conditions Modulate the Composition and Mechanical Properties of Tissue-Engineered Cartilage, Journal of Bone and Joint Surgery, 17, 130-138.

Wayne JS (1995) Load Partitioning Influences the Mechanical Response of Articular Cartilage, Annals of Biomedical Engineering, 23, 40-47.

Wayne JS (2008) Articular Cartilage Biomechanics, Informa Helthcare, New York.

Whiteside R A, Jakob RP, Wyss UP and Mainil-Varlet P (2005) Impact loading of articular cartilage during transplantation of osteochondral autograft, Journal of Joint and Bone surgery, 87-B, 1285-1291.

Wilson W, Driessen NJB, van Donkelaar CC and Ito KD (2006) Prediction of collagen orientation in articular cartilage by a collagen remodelling algorithm, Journal of Osteoarthritis and Cartilage, 14, 1196-1202.

Wu JZ and Herzog WU (2002) Elastic anisotropy of articular cartilage is associated with the microstructures of collagen fibres and chondrocytes, Journal of Biomechanics, Volume 35, Issue 7, July 2002, Pages 931-942.

Zeytin S, Konduk BA, Ipek M, Bindal C, Ucisik AH (2002) An evaluation of human articular cartilage on femoral head, Journal of Materials Science & Engineering, C 20, 219-222.

10. Appendices

10.1. Design diagrams

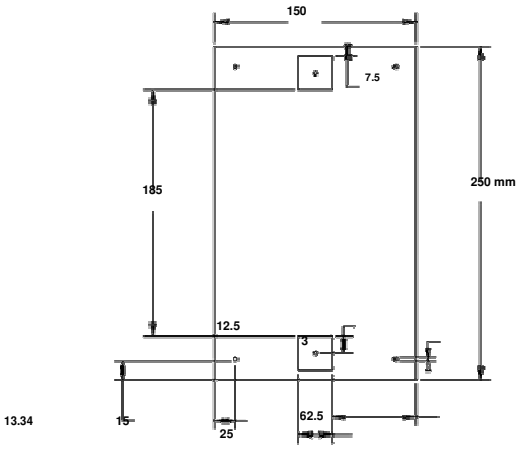

Figure 10.1: Base section

All measurements in mm.

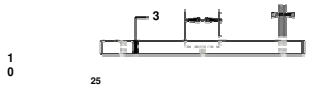

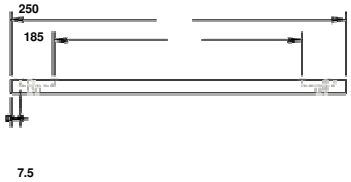

Figure 10.2: Left side support

All measurements in mm

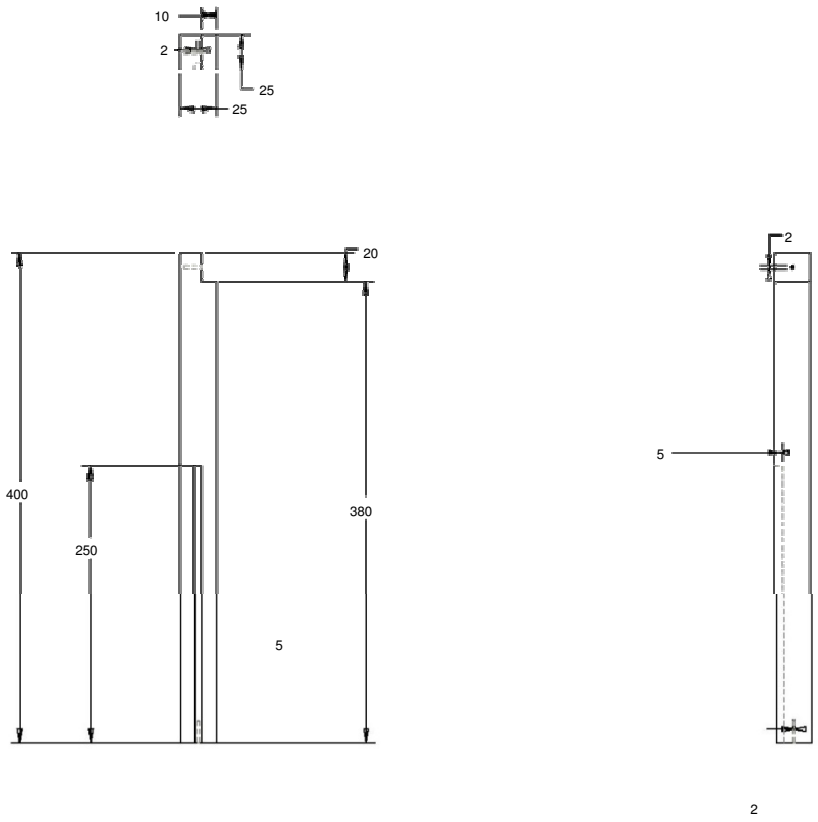

Figure 10.3: Right side support

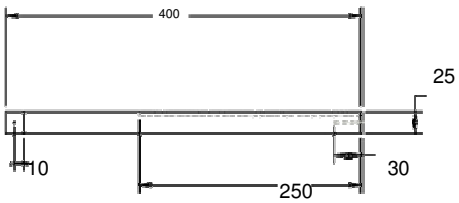

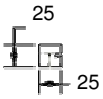

Figure 10.4: Tissue placing plate

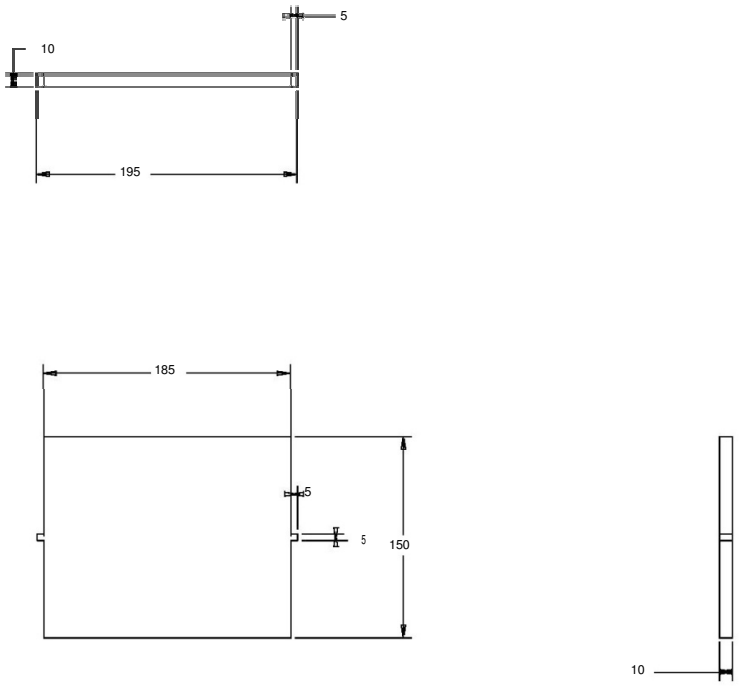

Figure 10.5: Top Plate for fixing the actuator

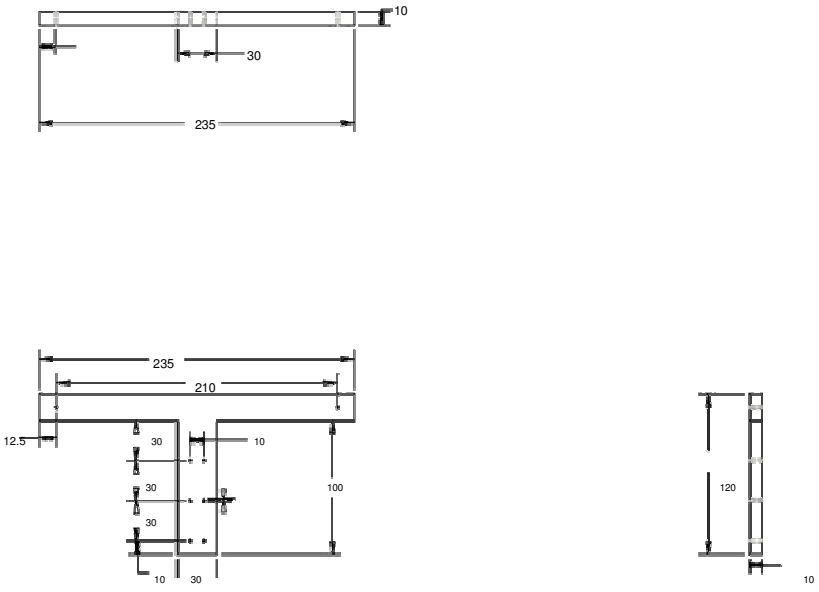

10.2. Matlab program code

```
% ********************************************************************
% This program was written by Phil Riches, University of Strathclyde.  %
% It simultaneously moves a linear actuator (KUMINA) and reads data from  %
% a LVDT through the DATAQ DI-194RS daq box.  %
% 18 August 2009  %
%  %
% This file requires the following functions:  %
%  %
% send_cmd.m  %
% relative_position_ramp.m  %
% delay.m  %
% decode_buffer.m  %
% stage_location.m  %
% kumi_home.m  %
%********************************************************************

% Ddetermine whether COM ports are open or not.
% They will be open if the program crashed previously.
% If they are open, close them.

if exist('s1') == 1
   fclose(s1);
   delete(s1);
   clear s1;
end;

if exist('s2') == 1
   fclose(s2);
   delete(s2);
   clear s2;
end;
```

```
% Clear all memory and close all figures

clear all
close all
warning off;

% Prepare an output csv file for writing

fname='daq_out';
fno = 0;
fext = '.csv';
fid = -1;

while fid == -1
   file_name = strcat(fname,num2str(fno),fext);
   fid = fopen(file_name,'w');
   fno = fno+1;
end;

% define excel output file name

file_name2 = strrep(file_name,fext,'.xls');

% Define the COM ports for the KUMINA and DI-194RS

com_kumi = 'COM4';
com_daq = 'COM3';

% Set sample rate at 60 Hz, since all channels collecting from DAQ

fs = 60;

% Look at dip swithces on back of KUMINA control box. Dip swith 3 is the second from the
left
```

```
% If the dip swith is up, then the actuator does 2500 pulses per mm
% If the dip swith is down, then it does 500 pulses per mm

ds_in = input('Is dip switch 3 up (1) or down (2)? [1]:');
if isempty(ds_in)
   ds = 'up';ppm = 2500;
elseif ds_in == 1
   ds = 'up';ppm = 2500;
elseif ds_in == 2
   ds = 'down';ppm = 500;
else
   ds = 'up';
end;

% specify which channel on the DI-194RS is to be read. This speeds up the
% reading routine.

channel = input('What channel of the DI-194RS is the lvdt plugged into? [1]: ');
if isempty(channel)
   channel = 1;
end;

% Do you want to calibrate?

calib = input('Do you want to calibrate (y/n) [n] : ','s');
if isempty(calib)
   calib = 'n';
end;

% if not, load the calibration file

if strcmp(calib,'n') == 1
   load('calib.mat');
else
```

```
    calib = 'y';
    savefile= 'calib.mat';
end;


if strcmp(calib,'n') == 1

    % Input ramp conditions and get the number of pulses required for the ramp

    ramp_depth = input('Ramp to (mm) [5] :');
    if isempty(ramp_depth)
        ramp_pulse = 5*ppm;
    elseif ramp_depth >= 0
        ramp_pulse = ramp_depth*ppm;
    else
        disp('Can''t do negative ramp');
        ramp_pulse = 0;
    end;

    ramp_pulse = round(ramp_pulse); % makes sure the number of pulses is an integer.

    % Input ramp velocity conditions and determined the required pulses per second

    ramp_vel = input('Ramp velocity (mm/s) [5] :');
    if isempty(ramp_vel)
        ramp_v = 5*ppm;
    elseif ramp_vel >= 0
        ramp_v = ramp_vel*ppm;
    else
        disp('Can''t do negative ramp velocity');
        ramp_v = ppm;
    end;

    ramp_v = round(ramp_v); % makes sure the pulse velocity is an integer.
```

```
    % Input hold conditions

    hold_time = input('Hold time (s) [30] :');
    if isempty(hold_time)
        hold_time = 30;
    elseif hold_time < 0
        disp('Can''t do negative hold. Setting to zero.');
        hold_time = 0;
    end;
else

    % Set calibration parameters

    ramp_pulse = 8*ppm; % 8mm ramp
    ramp_v = ppm; % 1 mm/s
    hold_time = 0;
    end;

% determine how long the ramp phase will take

ramp_time = ramp_pulse/ramp_v;
ramp_t = 1/fs:1/fs:ramp_time;
ramp_t = ramp_t';
srt=size(ramp_t,1);

% Work out total time of test

total_time = ramp_time + hold_time;
size_j = (total_time + 1)*60; % add one second for good measure

% Set spring contant of lvdt

spring_const = 0.131; % N/mm
```

```
% Set communication settings for KUMINA and DI-194RS

brate = 19200;
dbits = 8;
sbits = 1;
parbit = {'none'};
in_buf_siz = round(1.2*total_time*fs*8);
% in_buf_siz = 1024;

accel = 10;
data_len = 8;

%Actuator port s1 and dataq port s2

s1 = serial(com_kumi,...
    'BaudRate',brate,...
    'DataBits',dbits,...
    'StopBits',sbits,...
    'Parity','none',...
    'Timeout',0.1);

s2 = serial(com_daq,...
    'BaudRate',4800,...
    'DataBits',8,...
    'StopBits',1,...
    'Parity','none',...
    'Timeout',5,...
    'FlowControl','none',...
    'InputBufferSize',in_buf_siz,...
    'ReadAsyncMode','continuous');
% Define DAQ commands

stop_cmd  = ['00';'53';'30'];
start_cmd = ['00';'53';'31'];
```

```
sn_cmd    = ['00';'4E';'5A']; %serial number
reset_cmd = ['00';'52';'5A'];
all_chan  = ['00';'43';'3F'];
dig_chan  = ['00';'44';'30'];
init_cmd  = ['00';'42';'01'];

rd_ln = [1 1 1];
rd_ln2 = [1 1 11];

%*****************************************************
% Open and prepare the DAQ serial port

fopen(s2)

% Power down DTR and RTS and wait 100ms

set(s2,'DataTerminalReady','off',...
   'RequestToSend','off')
delay(0.01);

% Power up DTR and RTS and wait 100ms

set(s2,'DataTerminalReady','on',...
   'RequestToSend','on')
delay(0.01);

% Execute initialisation commands, mimicking WinDaq.

disp('Initialising DI-194RS');
A = send_cmd(s2,init_cmd,rd_ln);
B1 = send_cmd(s2,stop_cmd,rd_ln);
B2 = send_cmd(s2,sn_cmd,rd_ln2);
B3 = send_cmd(s2,all_chan,rd_ln);
B4 = send_cmd(s2,dig_chan,rd_ln);
```

```
disp('Done!');

%*****************************************************
% Open and prepare the KUMINA

disp('Initialising KUMINA');
fopen(s1);

% Say hello

fprintf(s1,'%s\r\n','SW,100,1000,100,100,1000,100');
out1 = fscanf(s1);

% Check to see if connected, stop if not.

if isempty(out1)
   disp('Kumina not ready');
   fclose(s1);
   fclose(s2);
   delete(s1);
   delete(s2);
   clear s1;
   clear s2;
   break;
elseif strcmp(out1(1),'K') == 1
   disp('Kumina connected');
else
   disp('Connected, but weird. Stopping.');
   break;
end;

% Set finding contact ramp conditions (fast and long)

in_contact = 0;
```

```
rvel = 2*ppm; % 2 mm/s
pul = 8*ppm; % 8 mm

disp('Finding contact...');

% start data acquisition

B5 = send_cmd(s2,start_cmd,rd_ln);

% read first byte of data and get rid - not necessary and messes up
% subsequent columns.

% tmp = fread(s2,1,'uint8');
% clear tmp

% start KUMINA on a relative ramp

[t3,loc3] = relative_position_ramp(s1,pul,rvel,accel);

while in_contact == 0

   % How many bytes are available?

   byt = s2.BytesAvailable;

   % If less than 8 bytes are available, keep looping

   while byt < 8
      byt = s2.BytesAvailable;
   end;

   % How many multiples of eight bytes are available?

   di = floor(byt/8);
```

```
% get each multiple of eight data from daq, process and output to file

for i = 1:di
   daq_out(1,1:8) = fread(s2,[1 8],'uint8');
   chan = decode_buffer(daq_out(1,1:8),channel);
   volts = -10 + (20/1023)*chan;

   % If it's the first data point, record it as such

   if exist('init_volts') == 0
      init_volts = volts;
   end;

   % Is there contact? i.e. has the lvdt moved?

   if abs(volts - init_volts) > 20/1023

      % Execute emergency stop

      fprintf(s1,'%s\r\n','TW');
      out = fscanf(s1);

      % specify that contact has been made

      in_contact = 1;
   end;

   % exit for loop if in contact

   if in_contact == 1
      break;
   end;
end;
```

```
end;

disp('Contact detected');

% Need to wait for the KUMINA to be ready again
% This is done by repeatedly asking for its location until an R appears as
% the last character in the output.

ready='B';
while strcmp(ready,'R') == 0
    [contact_loc,rem] = stage_location(s1);
    rem = strtrim(rem);
    srem = size(rem,2);
    ready = rem(1,srem);
end;

% Copying what the KUMINA software does.

fprintf(s1,'%s\r\n','SW,1,0,100,1,0,100');
out = fscanf(s1);

%**********************************

clear volts daq_out chan init_volts

% Set test variables

old_time = -1/fs;
time = 0;
old_loc = contact_loc;
stage_loc = contact_loc;
hold_phase = 0;
j = 2;
data_all(1,1:8) = 0;
```

```
disp('Ramping...');

% Dump stuff in DAQ buffer

byt = s2.BytesAvailable;
di = floor(byt/8);
tmp = fread(s2,[8 di],'uint8');
tmp = tmp';

% start KUMINA moving

[t3,loc3] = relative_position_ramp(s1,ramp_pulse,ramp_v,accel);

while size(data_all,1) < size_j

   % How many bytes are available?

   byt = s2.BytesAvailable;

   % If less than 8 bytes are available, keep looping

   while byt < 8
      byt = s2.BytesAvailable;
   end;

   % How many multiples of eight bytes are available?

   di = floor(byt/8);

   % get block of data

   daq_out = fread(s2,[8 di],'uint8');
   daq_out = daq_out';
```

```
    data_all = cat(1,data_all,daq_out);

    clear daq_out data_out kumi_out;

end;

% Clear important variables

clear time volts loc;

% Remove the first line of data, since this is just zeros

sda = size(data_all,1);
data_all = data_all(2:sda,1:8);
sda = sda-1;

% Ste the time variable

time = 1/60:1/60:sda/60;
time = time';

% Determine the voltage from the lvdt using the decode_buffer function

for i = 1:sda
    chan = decode_buffer(data_all(i,1:8),channel);
    volts(i,1) = -10 + (20/1023)*chan;
end;

% Determine the time index at which the kumina starts moving. This is done
% by determining whether the lvdt changes voltage or not.

for i = 2:sda
    if volts(i,1) < volts(i-1,1)
```

```
        contact_index = i;
        break;
    end;
end;

% Find the end of the ramp phase and beginning of hold phase

hold_index = contact_index + srt;
if hold_index > sda
    hold_index = sda;
end;

% Estimate stage location in mm

loc(1:contact_index-1,1) = 0;
loc(contact_index:hold_index-1,1) = ramp_t*ramp_v/ppm;
loc(hold_index:sda,1) = ramp_pulse/ppm;

% Stop reading DAQ

B6 = send_cmd(s2,stop_cmd,rd_ln);

% Send the actuator back to zero

kumi_home(s1);

% Handshake

fprintf(s1,'%s\r\n','SW,1,0,100,1,0,100');
out = fscanf(s1);

% If calibrating, fit a regression and save the resulting polynomial coefficients

if strcmp(calib,'y') == 1
```

```
    % fit 2nd order regression (quadratic)

    p = polyfit(volts,loc,2)

    % determine best fit

    fit_loc = polyval(p,volts);

    % plot calibration curve

    figure
    plot(volts,loc);
    hold on
    plot(volts,fit_loc,'r');
    xlabel('volts');
    ylabel('displacement (mm)');

    % save calibration data

    save(savefile,'p');
end;

% If not calibrating, work out the surface displacement and output to xls
% file.

if strcmp(calib,'n') == 1

    % determine lvdt displacement from calibration data

    lvdt_loc = polyval(p,volts);

    % find the force in the spring
```

```
    force = spring_const * lvdt_loc;

    % find the surface displacement

    surface_displacement = loc - lvdt_loc;

    % Zero at start of hold phase

    surface_displacement = surface_displacement - surface_displacement(hold_index,1);
    time = time - time(hold_index,1);

    % determine the 3-parameter solid to fit adjusted so it goes through
    % origin. i.e. a two parameter solid

    surf_func3 = @(x)sum((surface_displacement(hold_index:sda,1) - x(1) + x(1).*exp(-
x(2).*time(hold_index:sda,1))).^2,1);
    vars3 = fminsearch(surf_func3,[1 1])

    % Find the best fit curve

    surf_fit3 = vars3(1) - vars3(1)*exp(-vars3(2)*time);

    % Plot the output

    figure
    subplot(3,1,1);

plot(time(hold_index:sda,1),surface_displacement(hold_index:sda,1),time(hold_index:sda,1),
surf_fit3(hold_index:sda,1));
    ylabel('Surface Displacement (mm)');
    xlabel('Time (s)');
    subplot(3,1,2);
    plot(time(hold_index:sda,1),lvdt_loc(hold_index:sda,1));
    xlabel('Time (s)');
```

```
    ylabel('lvdt displacement (mm)');
    subplot(3,1,3);
    plot(time(hold_index:sda,1),force(hold_index:sda,1));
    xlabel('Time (s)');
    ylabel('Force (N)');
    drawnow;

    % Export data to an xls sheet

    xls_data = cat(2,time,lvdt_loc,loc,surface_displacement,surf_fit3,force);
    columnHeader = {'Time', 'LVDT disp (mm)','Act disp (mm)','Surf disp (mm)','Surf fit
(mm)','Force (N)'};
    xlswrite(file_name2,columnHeader,'sheet2','A1');
       xlswrite(file_name2,xls_data,'Sheet2','A2');

end;

% close all connections

fclose(s1);
fclose(s2);
delete(s1);
delete(s2);
clear s1;
clear s2;

% Done.
% ************************************************************************
```

Send_cmd.m Subroutine program for communicating with DAQ

```
function [A] = send_cmd(s,in_cmd,read_length)
cmd = hex2dec(in_cmd);
```

```
lgth = length(cmd);
for i = 1:lgth
   fwrite(s,cmd(i),'uint8');
   %delay(0.1);
   if i > 1 % don't read after null character
      temp = fread(s,read_length(i));
      if temp == 255 % read error
         % try to read again after short delay
         delay(0.1);
         temp = fread(s,read_length(i));
      end;
      A{i-1} = char(temp);
   end;
end;
```

Relative_position_ramp subroutine program for detect whether inductor is contact is specimen surface or not. After contact it moves down wards from the contact position to user defined displacement.

```
function [t,loc] = relative_position_ramp(s,x,y,z)
init_command = strcat('S1,1,',num2str(y),',',num2str(z));
fprintf(s,'%s\r\n',init_command);
out = fscanf(s);

% Set command
if x >=0

   kumi_command = strcat('P1,+',num2str(x));
else
   kumi_command = strcat('P1,',num2str(x));
end;
% send command

fprintf(s,'%s\r\n',kumi_command);
```

```
out = fscanf(s);
fprintf(s,'%s\r\n','G');
outg = fscanf(s);
loc = str2num(strtok(outg,','));
finish = loc + x;

% Do the command

fprintf(s,'%s\r\n','D');
out = fscanf(s);

t=1;loc=1;
return;
```

Delay subroutine function used for to create user defined time delay while program running. The purpose of this function is speed matching between two devices.

```
function [] = delay(x);

t = timer('TimerFcn',';','StartDelay',x);
start(t);
wait(t);
delete(t);
return;
```

Decode_ buffer function used to determine the voltage from the lvdt.

```
function chan = decode_buffer(daq_out,chan)
% daq_out must contain 1 row and eight columns of 0-255 (8 bit) data
% Convert 0-255 to 8 bit binary representation (in a string)
str = dec2bin(daq_out,8);

% Take the most significant seven bits of one and put with the 3 most
% significant bits of the second channel to get a 10 bit binary number,
% which is then recoded back to decmial representation
```

```
chan = bin2dec(strcat(str(2*chan,1:7),str(2*chan-1,1:3)));
```

Stage_location subroutine function for find out the current position of the actuator

```
function [loc,rem] = stage_location(s)
try
   % send command to kumina to ask wher the stage is
      fprintf(s,'%s\r\n','G');

   % read response
      outg = fscanf(s);
      % convert response to location (in pulses from kumina zero)

      [locstr,rem] = strtok(outg,',');
   loc = str2num(locstr);

  catch % if there's an error, try it again
   try
      fprintf(s,'%s\r\n','G');
      outg = fscanf(s);
      [locstr,rem] = strtok(outg,',');
      loc = str2num(locstr);

   catch % and again
      try
        fprintf(s,'%s\r\n','G');
        outg = fscanf(s);
        [locstr,rem] = strtok(outg,',');
        loc = str2num(locstr);

      catch % and again
         try
            fprintf(s,'%s\r\n','G');
```

```
            outg = fscanf(s);
            [locstr,rem] = strtok(outg,',');
            loc = str2num(locstr);
         catch % give up and return loc = 0
            loc = 0
            % disp('Error in stage location');
         end;
      end;
   end;
end;
return;
```

Kumi_home subroutine function for send the actuator to home position.

```
function [t,loc] = kumi_home(s);

% Perform a 'HOME'

fprintf(s,'%s\r\n','SW,100,1000,100,100,1000,100');
out = fscanf(s);

fprintf(s,'%s\r\n','OW');
out = fscanf(s);

if strcmp(out,'X') == 1
   fprintf(s,'%s\r\n','OW');
   out = fscanf(s)
end;

if strcmp(out,'X') == 1
   fprintf(s,'%s\r\n','OW');
   out = fscanf(s)
end;

if strcmp(out,'X') == 1
```

```
    fprintf(s,'%s\r\n','OW');
    out = fscanf(s)
end;

if strcmp(out,'X') == 1
    fprintf(s,'%s\r\n','OW');
    out = fscanf(s)
end;

if strcmp(out,'X') == 1
    fprintf(s,'%s\r\n','OW');
    out = fscanf(s)
end;
% find stage location

% loc = stage_location(s);
% i = 1;
%
% while loc ~= 0
%     loc(i) = stage_location(s);
%     et(i) = toc;
%     tic;
%     i = i+1;
% end;
%
% t = cumsum(et);
t=1;loc=1;
```